

Late summer diatom biomass and community structure on and around the naturally iron-fertilised Kerguelen Plateau in the Southern Ocean

Leanne K. Armand*, Veronique Cornet-Barthaux, Julie Mosseri, Bernard Quéguiner

Aix-Marseille Université, CNRS, LOB-UMR 6535, Laboratoire d'Océanographie et de Biogéochimie, OSU/Centre d'Océanologie de Marseille, Marseille, France

Accepted 9 December 2007

Abstract

Analysis of the diatom assemblage during the recent *KErguelen*: compared study of *Ocean* and *Plateau* in Surface water (KEOPS) mission (January–February 2005), enabled a modern description of the summer bloom community over the Kerguelen Plateau in the context of the community in the surrounding high-nutrient, low-chlorophyll (HNLC) Southern Ocean waters. Net samples revealed biogeographic partitioning of certain species. Comparison of net samples with CTD-Niskin bottle samples revealed a considerable underestimation of large diatom species in the water samples. We analysed four plateau stations and one off-plateau HNLC station for individual species abundances and biomass contributions down to 150 m. The stations can be divided into two groups based on species composition and total biomass contributions, equating to high ($45.6\text{--}99.4\ \mu\text{g CL}^{-1}$) and low ($2.5\text{--}25.7\ \mu\text{g CL}^{-1}$) biomass regimes. Individual species abundances were not related to the major species biomass contributions. Repeat analyses at the bloom station, A3, and the off-plateau HNLC station, C11, revealed evolution from a *Chaetoceros* subgenus *Hyalochaete* bloom to a remnant *Eucampia antarctica* assemblage. In contrast the HNLC station, C11, remained dominated by *Fragilariopsis pseudonana* and *F. kerguelensis* throughout the survey. Comparison to artificial iron experiments reveals differences in the responses of *Pseudo-nitzschia* spp. and *F. kerguelensis*, which may arise in part from differences in macro-nutrient supply, in particular silicic acid availability, as well as from seasonal succession.

© 2008 Elsevier Ltd. All rights reserved.

Keywords: Diatoms; Bacillariophyceae; Biomass; Cell abundance; *Chaetoceros*; *Eucampia*

1. Introduction

The Kerguelen-Heard archipelago in the south Indian Ocean represents one of a handful of Subantarctic/Antarctic islands where early studies of phytoplankton were undertaken. Phytoplankton from Kerguelen-Heard was examined by Moseley on the H.M.S. *Challenger* and reported by O'Meara (1877), with 33 diatom species documented. Sporadic and somewhat decadal sampling from the 1950s through to recent times resulted in a list of 160 pelagic diatom species (Manguin, 1954; Ealey and Chittleborough, 1956; Kozlova, 1962; Steyaert, 1974;

Sournia et al., 1979; Fryxell, 1991; Blain et al., 2001; Kopczyńska and Fiala, 2003; Armand, pers. obs.). The KERFIX time series study southwest of Kerguelen Isles in high-nutrient, low-chlorophyll (HNLC) waters (Fiala et al., 1998; Kopczyńska et al., 1998) revealed the generally year-long impoverished state of the phytoplankton population, and ranked diatom biomass behind biomass contributions from pico/nanoflagellates and coccolithophorids. The KERFIX study nonetheless revealed the recurrent summer bloom was dominated by *Fragilariopsis kerguelensis* and *Thalassionema nitzschioides* in the HNLC waters southwest of Kerguelen Plateau.

Sullivan et al. (1993) first reported on the high chlorophyll concentrations over the Kerguelen Plateau from satellite images. A recent study on the north-eastern zone of the plateau led to the hypothesis that natural fertilisation processes sustain the bloom in this area (Blain

*Corresponding author at: ACE CRC, Private Bag 80, Hobart, Tasmania 7001, Australia. Tel.: +61 3 6226 1997; fax: +61 3 6226 2440.

E-mail addresses: leanne.armand@utas.edu.au, leanne.armand@acecrc.org.au (L.K. Armand).

et al., 2001; Bucciarelli et al., 2001). The *KE*erguelen: compared study of *Ocean and Plateau in Surface water* (KEOPS) programme (January–February 2005) focussed on the south-eastern bloom, positioned south of the Polar Front, between Kerguelen and Heard Islands. Oceanographic studies around Kerguelen and the Crozet Basins have been produced by Park et al. (1991, 1998), Park and Gambéroni (1995, 1997) and Charrassin et al. (2004). Studies detailing the oceanography pertinent to the KEOPS study are found in Park et al. (2008a, b), van Beek et al. (2008) and Mongin et al. (2008). Oceanographic processes in this region are dominated by tidal action across the plateau with large vertical diffusivities (Park et al., 2008a, b). MODIS satellite images indicated that the summer bloom had peaked prior to our survey period across the Kerguelen Plateau (Blain et al., 2007), and our study reflects a survey of the diatom community towards the end of the main bloom period. The related studies on the heterotrophic communities were made by Carlotti et al. (2008), Christaki et al. (2008) and Obernosterer et al. (2008).

The objective of our study was to quantify the diatom community and to examine the physical and/or chemical factors potentially regulating diatom growth and species composition. The sampling programme included regions within and exterior to the major spring bloom to reflect conditions within an iron-replete zone and characterised by HNLC conditions. We provide the qualitative (net hauls) and quantitative (CTD) assessment of diatoms encountered including their individual species contribution in terms of biomass. Finally, we document the evolving community composition at two repeat stations representative of conditions within the iron-replete bloom and outside the plateau in the HNLC off-plateau region.

2. Materials and methods

2.1. Study area and physical–chemical characteristics

We illustrate the position of our sample sites in Fig. 1 and list their locations in Table 1. MODIS satellite images indicate that the bloom over the Kerguelen Plateau formed in early November 2004 and concluded in late February 2005 (Blain et al., 2007; Mongin et al., 2008). The mean physical and chemical characteristics pertinent to the diatom distribution in the surface waters at these locations are summarised in Table 2. Surface waters above the plateau were slightly warmer and had shallower euphotic depths as compared to the off-plateau locations. Transect A stations, on average, had 1% photosynthetically active radiation (PAR) at 45 m depth, transect B stations had an average 1% PAR at 81 m depth, whereas the C transect PAR was 102 m for 1% PAR. Chl *a* and fucoxanthin values representative of phytoplankton concentrations in the surface waters show clearly the difference between the water on and off the plateau, while the difference is less marked for the biogenic silica concentrations. Mosseri

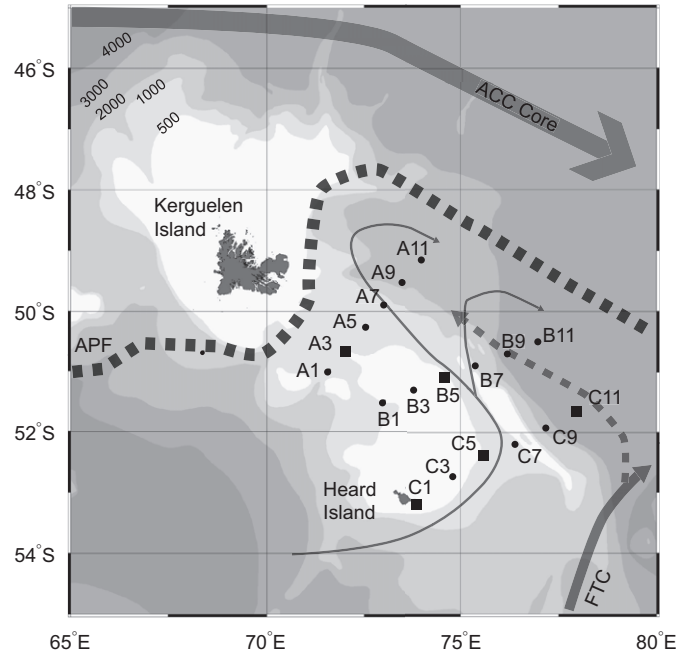


Fig. 1. KEOPS station locations. Net hauls were made at all stations. CTD diatom samples were taken at the five station locations indicated by squares. Station A3 and C11 were repeat reference stations within and exterior to the plateau-based phytoplankton bloom, respectively. Currents and fronts from Park et al. (2008b, Fig. 11). APF: Antarctic Polar Front; ACC Core: Antarctic Circumpolar Current core; FTC: Fawn Trough Current; Thin black lines over plateau indicate flow through the Heard/MacDonald Islands Trough. Bathymetry in metres. Plotted using ODV (Schlitzer, 2006).

et al. (2008) described diatoms located off-plateau as more highly silicified than those on the plateau as observed in high silica to nitrate and carbon uptake ratios. This is consistent with an increased percentage of senescent cells (see Results), thus contributing to the difference in observations across these parameters, and also given that the Chl *a* and fucoxanthin contributions are not solely diatom-derived (Jeffery et al., 2005). Nutrient surface distributions are presented in Mosseri et al. (2008). The off-plateau waters were NO_3 and silicate-rich, yet in spite of the particularly low silicic acid surface values ($< 2 \mu\text{M}$) above the Kerguelen Plateau these authors show depleted silicic acid concentrations at the surface were close to growth limiting in the KEOPS study. Blain et al. (2008) indicate that dissolved iron concentrations in the surface waters were constant across the plateau stations with a mean of 0.09 nM. The value observed off-plateau was not significantly different with a mean of 0.073 nM. Deep-water iron concentrations differed between the plateau and off-plateau deep waters (e.g., at 400 m: mean Fe concentration values were 0.3 nM above the plateau and 0.11 nM off-plateau). There was an elevated upward flux on the plateau due to an increased exchange with subsurface waters below the mixed-layer depth (MLD) (Blain et al., 2007, 2008).

Table 1
Locations of net hauls and CTD stations

Station	Code	Date	Latitude	Longitude	Depth (m) ^a	Mesh size (μm)
<i>Net Hauls</i>						
A1	ZN 007	23/1/05	51°00.00'S	71°35.80'E	200	330
A3a	ZN 001	18/1/05	50°37.80'S	72°04.80'E	200	330
A3b	ZN 006	23/1/05	50°37.90'S	72°04.70'E	200	330
A3c	ZN 008	23/1/05	50°40.90'S	71°59.70'E	200	330
A3d	ZN 010	24/1/05	50°43.23'S	72°00.95'E	200	330
A3e	ZN 023	4/2/05	50°38.52'S	72°03.43'E	50	53
A3f	ZN 033	12/2/05	50°37.89'S	72°03.97'E	100	53
A3g	ZN 034	12/2/05	50°32.10'S	72°04.20'E	100	53
A5	ZN 005	22/1/05	50°15.60'S	72°34.00'E	200	330
A7	ZN 004	22/1/05	49°53.40'S	73°02.35'E	200	330
A9	ZN 003	21/1/05	49°31.50'S	73°30.90'E	200	330
A11	ZN 002	20/1/05	49°09.03'S	74°00.06'E	200	330
B1	ZN 021	2/2/05	51°30.00'S	73°00.00'E	50	53
B3	ZN 020	2/2/05	51°17.82'S	73°47.46'E	50	53
B5	ZN 019	2/2/05	51°05.90'S	74°35.80'E	50	53
B7	ZN 018	30/1/05	50°53.80'S	75°23.35'E	50	53
B9	ZN 017	30/1/05	50°41.80'S	76°12.10'E	50	53
B11	ZN 016	29/1/05	50°30.30'S	76°59.10'E	50	53
C1	ZN 030	9/2/05	53°11.27'S	73°53.37'E	50	53
C3	ZN 029	8/2/05	52°41.25'S	74°45.45'E	50	53
C5	ZN 027	7/2/05	52°22.70'S	75°34.90'E	50	53
C7	ZN 026	7/2/05	52°11.30'S	76°23.50'E	50	53
C9	ZN 025	6/2/05	51°55.05'S	77°12.01'E	50	53
C11a	ZN 011	26/1/05	51°38.80'S	78°00.00'E	200	330
C11b	ZN 012	26/1/05	51°37.80'S	77°58.00'E	200	330
C11c	ZN 013	27/1/05	51°38.90'S	78°59.90'E	70	53
C11d	ZN 014	28/1/05	51°39.05'S	77°59.81'E	80	53
C11e	ZN 024	5/2/05	51°39.10'S	78°00.00'E	50	53
Station	Code	Date	Latitude	Longitude	Depth (m) ^b	
<i>CTD Niskin samples</i>						
A3-1	CTD 007	19/1/05	50°37.80'S	72°04.60'E	10, 50	
A3-3	CTD 031	24/1/05	50°41.30'S	71°59.90'E	10, 60, 100	
A3-4	CTD 076	4/2/05	50°39.50'S	72°04.00'E	10, 60, 100	
A3-5	CTD 112	12/2/05	50°37.79'S	72°05.29'E	10, 60, 100	
B5	CTD 064	2/2/05	51°05.70'S	74°35.80'E	10, 30, 60, 100	
C1	CTD 102	9/2/05	53°11.32'S	73°51.74'E	10, 50, 70, 134	
C5	CTD 094	8/2/05	52°22.09'S	75°36.52'E	30, 50, 80, 150	
C11-1	CTD 040	26/1/05	51°37.50'S	77°57.40'E	20, 50, 80, 150	
C11-2	CTD 045	28/1/05	51°38.80'S	78°00.10'E	10, 50, 80, 150	
C11-3	CTD 082	6/2/05	51°39.00'S	78°00.00'E	10, 50, 80, 150	

^aNets were hauled from these depths.

^bDiscrete water depth sampled.

2.2. Diatom sampling

Qualitative sampling of surface waters was undertaken on 21 net haul samples over the KEOPS A-C transects on the eastern plateau region between Kerguelen and Heard islands (Fig. 1 and Table 1). Nets were either 330 or 53 μm in mesh size and collected using a Bongo two-net system, from the chlorophyll maximum depth to the surface. These net hauls were designed for zooplankton sampling (densities, respiration and gut content; Carlotti et al., 2008) and the volume of water filtered by the nets was not determined. Three to 10 mL of the netted sample were

generally observed in an Utermöhl style counting chamber (over at least half of the base) within 1 h (max. 24 h) under a Nikon Eclipse TE200 inverted microscope at × 10, × 20 or × 40 magnification. Species abundance observations were divided into the following arbitrary categories: d = dominant (observed in all fields of view, major contributor/s), c = common (observed in most fields of view), m = minor (observed less than 15 times in a sample), r = rare (observed once or twice in a sample).

Quantitative sampling at discrete water depths within the upper 150 m of the water column was taken from 24 Niskin bottles on a rosette frame equipped with a *Sea Bird*

Table 2
Mean properties in surface waters from studied stations

Station	Sea surface temp. (°C) ^a	Sea surface salinity ^a	1% PAR depth (m) ^a	Bsi (μmol L ⁻¹) ^b		
<i>Net Hauls</i>						
A1	3.77	33.86	39.7	3.76		
A3a	3.53	33.46	41.8	3.39		
A3b	3.53	33.86	48	2.61		
A3c	3.66	33.86	25.8	5.74		
A3d	3.81	33.86	40.7	nd		
A3e	3.78	33.87	46.9	nd		
A3f	3.96	33.88	48.4	Nd		
A3g	nd	nd	58	Nd		
A5	3.58	33.86	53.9	1.09		
A7	3.34	33.85	49.8	1.5		
A9	3.41	33.53	nd	0.8		
A11	3.75	33.59	nd	0.9		
B1	3.68	33.87	47.5	4.15		
B3	3.3	33.86	131.4	3.04		
B5	3.09	33.87	39.9	2.96		
B7	3.12	33.87	107.1	0.97		
B9	2.85	33.89	nd	1.45		
B11	2.08	33.77	nd	nd		
C1	2.73	33.84	nd	Nd		
C3	2.61	33.84	105	1.66		
C5	2.78	33.85	82.6	1.25		
C7	2.73	33.85	nd	1.62		
C9	2.84	33.86	nd	2.39		
C11a	1.92	33.80	97.5	2.78		
C11b	Nd	nd	nd	nd		
C11c	Nd	nd	nd	nd		
C11d	1.82	33.78	nd	4.6		
C11e	3.34	33.88	122.9	3.35		
Station	Sea surface temp. (°C) ^a	Sea surface salinity ^a	1% PAR depth (m) ^a	Bsi (μmol L ⁻¹) ^b	Total Chl <i>a</i> (μg L ⁻¹) ^c	Fuco. (μg L ⁻¹) ^c
<i>CTD Niskin samples</i>						
A3-1	3.5	33.56	41.8	3.39	0.94	0.56
A3-3	3.68	33.86	39.9	5.74	0.97	0.63
A3-4	3.58	33.86	46.0	1.26	1.34	0.51
A3-5	3.84	33.88	43.8	2.24	1.09	0.59
B5	3.09	33.87	39.9	2.96	1.32	0.77
C1	2.6	33.84	nd	4.01	0.41	0.17
C5	2.76	33.85	82.6	1.25	0.32	0.09
C11-1	1.91	33.80	97.5	18.43	0.22	0.10
C11-2	1.72	33.79	97.5	4.6	0.17	0.09
C11-3	1.91	33.80	122.9	3.35	0.16	0.07

nd: no data.

^aSea-surface temperature, salinity and photosynthetically available radiation data from KEOPS community.

^bBsi from Mosseri et al. (2008).

^cChlorophyll *a* and Fucoxanthin from Uitz et al. (submitted).

SBE-911 plus CTD sensor. Aliquots of 125 mL were preserved with acid Lugol's iodine solution (final concentration of 0.32%) and stored in coloured glass bottles, in the dark and at room temperature, until their analysis on return to the laboratory.

2.3. Microscopy and taxonomy

Diatoms were identified to the lowest possible taxonomic level, enumerated, and their linear dimensions documented

under a Nikon Eclipse TE2000-E inverted microscope equipped with phase-contrast and a long distance condenser. Diatoms were enumerated from a 10-mL subsample after settling for 24 h in an Utermöhl style counting chamber. Counts were made from the entire chamber following the Utermöhl methodology (Hasle, 1978) for all samples at stations A3 and C11. Samples from stations B5, C1 and C5 were concentrated by settling 25–100 mL of a sample for 48 h in the dark to a final volume of 10 mL. One microlitre of the homogenised concentrate was placed in a

Sedgwick–Rafter counting chamber for enumeration. The procedure of Guillard (1978) and Hötzel and Croome (1998) was followed, whereby the diatoms within 250–500 squares (1 sq = 1 μ L) were enumerated, approximating to 500–1200 cells. We identify “dead cells” in this study as those that we considered as empty frustules devoid of internal contents visible to the eye during microscopy. This includes single cells and those that occurred within chains. We did not include, nor enumerate, clearly broken or ingested cells within this dead cell category.

Taxonomy followed modern concepts in Hasle and Syvertsen (1997). All species authorships are listed in Appendix 1 (supplementary material). Several taxa groupings were made due to the difficulty in differentiating some species. We grouped all small *Chaetoceros* species of the subgenus *Hyalochaete* together although the dominant contributor was *Chaetoceros socialis*. We hereafter refer to this group as *Chaetoceros Hyalochaete* spp. *Chaetoceros* resting spores from the subgenus *Hyalochaete* are poorly known to species level and so were grouped. We employed the *Chaetoceros bulbosum* complex (Ehrenberg) Heiden to include all reported synonyms in this region of *C. atlanticus* Cleve, *C. atlanticus* var. *neapolitana* (Schroder) Hustedt, *C. atlanticus* var. *skeleton* (Schütt) Hustedt and *C. bulbosum* Ehrenberg. *Fragilariopsis rhombica* and

F. separanda could not be distinguished and so were grouped. *Membraneis imposter* and *M. challengerii* and species of the genera *Banquisia*, *Manguinea* and *Plagiotropis* represent species of the *Membraneis* spp. category. These diatoms were often undergoing division, making exact species identification difficult (images available on request). *Navicula directa* and a smaller unidentified *Naviculaceae* species represent the category *Navicula* spp. The genus *Pseudo-nitzschia* was divided into two categories based on the shape and width of the transapical axis (above and below 5 μ m). Specimens with a transapical axis > 5 μ m are dominated by the species *P. heimii*, whereas *P. lineola*, *P. turgidula* and *P. subcurvata* species were encountered in the < 5- μ m category. Chain-forming pennates predominantly in girdle view were assembled under Other Pennates. Other Centrics in general contained small specimens (< 10 μ m in diameter) that we considered attributable to the genus *Thalassiosira*, particularly *T. frenguelli* and *T. gracilis* var. *gracilis*. Finally, we divided *Eucampia antarctica* v. *antarctica* cells into three categories based on the cell's frustule structure (Fig. 2). We consider typical cells those normally reported in the literature, i.e. heavily silicified, asymmetric cells that form coiling chains. Atypical cells were divided into two categories, the first representing one typical cell with an attached sibling cell (or two) that

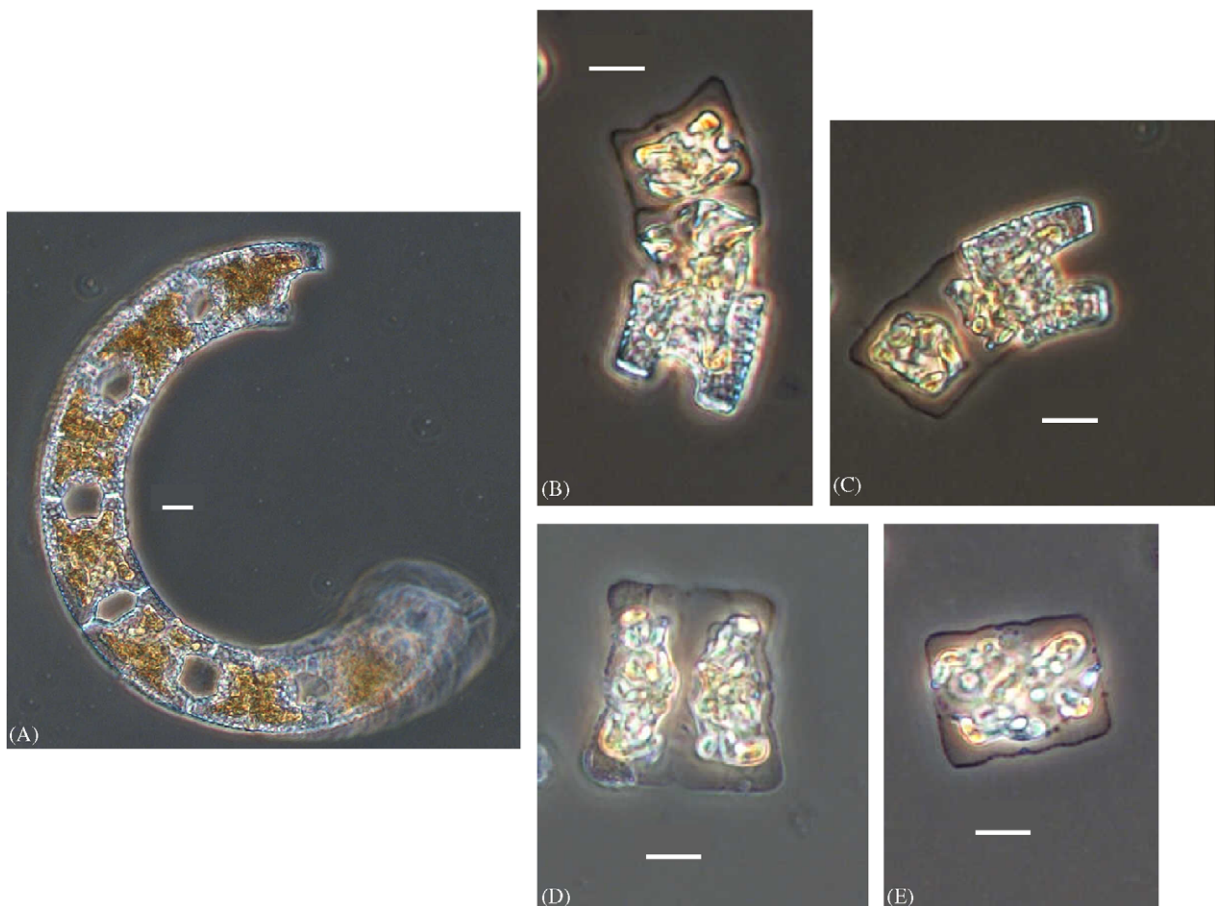


Fig. 2. Micrographs of variation in *Eucampia antarctica* var. *antarctica*: (A) typical coiling chain, (B and C) form 1 atypical cells, (D and E) form 2 atypical cells. Scale bar in all images is 10 μ m.

appeared lightly silicified, the second, representing a single lightly silicified and un-ornamented cell. All atypical cell measurements are reported as combined values.

2.4. Biomass

Methodology for the derivation of linear measurements, biovolume measurements and biomass calculations for individual species or groupings based on this study are presented elsewhere (Cornet-Barthaux et al., 2007). We use the definitions defined within that work to classify a specific diatom species' biomass contribution as small ($<85 \text{ pg C cell}^{-1}$), intermediate ($85\text{--}488 \text{ pg C cell}^{-1}$) and large ($>488 \text{ pg C cell}^{-1}$). Biomass does not include a correction for vacuole size in our diatom species. The calculation of an integrated biomass for each CTD sample data was determined by the multiplication of the MLD by the biomass extrapolated for this depth. All standing stocks per m^2 described herein are trapezoidal depth-integrated values for the water column between the surface and MLD.

3. Results and discussion

3.1. Net hauled material

During this study 58 species or groupings were encountered by net hauls (Appendix 2 supplementary material). At each of the 21 stations between 16 and 32 species were noted. We tabulate the 18 most common or dominant diatoms in Table 3. The dominant diatom across almost every station was the long needle-shaped and colony-bundled *Thalassiothrix antarctica*, followed by the ribbon-chained *F. kerguelensis*. Half way through the experiment the mesh size had to change from 300 to $53 \mu\text{m}$ due to net damage and therefore small-sized diatoms were under represented in net samples during the initial sampling period. Results from net hauls therefore only represent gross findings. This aside we identified large-sized diatom contributions in certain transects or regions of the Kerguelen Plateau, as follows:

- (i) *Species present at all stations*: Fifteen species were noted as ubiquitous across all stations. Their geographic distributions could be divided in three. Firstly, species such as *T. antarctica* (dominant), *Dactyliosolen antarcticus* (common), *C. bulbosum* complex (minor) and *Chaetoceros dictyota* (rare) were observed at all stations with generally the same intensity. Secondly, another group increased in presence off-plateau, such as *Asteromphalus hookerii*, *Pseudo-nitzschia* spp. and *Thalassiosira tumida*. The third group showed a tendency for greater concentrations on the plateau. These included *Corethron inerme* and *Rhizosolenia* spp. (e.g. *R. simplex*, *R. antennata* f. *semispina*), *F. kerguelensis* (most dominant along Transect B), *Nitzschia* spp. (most common along Transect A), *Proboscia alata* and *P. inermis* (Transect A and

Transect B dominant, respectively), *Membraneis* spp. (greatest occurrence at station C3) and *Rhizosolenia chunii* (a rare to minor contributor, most common at Stations B7 and B9).

- (ii) *Species observed predominately, or only, at plateau stations*. Background species (rare to minor appearances) such as *Actinocyclus* spp., *Chaetoceros dictyota*, *Dactyliosolen tenuijunctus* and *Odontella weissflogii* occurred on the plateau. *Coscinodiscus* spp. were more common on the plateau in minor occurrences than off the plateau, where they appeared rarely or were absent. *E. antarctica* v. *antarctica* (as curling chains in net hauled material) were a common constituent at all stations but were observed rarely, or in minor abundances, at stations off-plateau. The species *Guinardia cylindrus* (common), *Chaetoceros convolutus* (A5 and A7 rare) and *Pseudo-nitzschia heimii* occurred principally in samples over Transect A, being rare to absent at other stations. *Rhizosolenia polydactyla* f. *polydactyla* was rare to absent in most stations but was common at station C1 near Heard Island. *Thalassiosira lentiginosa* was largely absent from Transect A stations and in greater appearance at Transect B and C stations, being curiously dominant at station C1.
- (iii) *Species observed predominately, or only, at stations off-plateau*: *Azpeitia tabularis*, *Nitzschia sicula* v. *rostrata* and *Chaetoceros adelanum* were present as rare to minor background taxa at stations off the plateau. The strongly silicified winter stage of *Thalassiosira oliverana* (Fryxell, 1994, not to be confused with the synonym *T. maculata* otherwise considered the summer stage of *T. oliverana*), was present as a common contributor in more off-plateau located stations, whereas the large and thinly silicified *Porosira pseudodenticulata* was only encountered at Station C11.

3.2. Quantitative diatom survey

Our results focus on the relative abundance of all diatom species encountered (biocoenose and thanatocoenose) and the living biomass composition. The complete dataset can be found in Appendix 3 (supplementary material). Overall results are summarised in Fig. 3, and diatom biomass in Figs. 4–6. The total diatom biomass ranged more than 10-fold from an average of $7 \mu\text{g C L}^{-1}$ at Stations C5 and C1 to $99.4 \mu\text{g C L}^{-1}$ at Station A3 (12 February 2005, Table 4).

3.2.1. Station A3

At the start of our study, $>75\%$ of the cells encountered were viable within the surface 100 m (Fig. 3A), but an increase in the number of senescent cells was observed on the 4 February at both 10 and 60 m depths. The species contributing to this increase in non-living cells were *Thalassionema nitz.* f. *nitzschoides* (2% rel. abund.), *F. kerguelensis* (2%) and *E. antarctica* (typic cells, 8%). The increase in non-living material at 100 m on the last visit

Table 3
Dominant diatom species from net hauls

Transect station no.	Code	No. species	<i>Asteromphalus hookeri</i>	<i>Chaetoceros bulbosum</i> complex	<i>C. inermis</i>	<i>Coscinodiscus</i> spp.	<i>Diacyclops antarcticus</i>	<i>Eucampia ant. antarctica</i>	<i>Fragilariopsis kerguelensis</i>	<i>Gamardella cylindrus</i>	<i>Navicula</i> spp.	<i>Porosira pseudolenticulata</i>	<i>P. alata</i>	<i>P.-a. helmii</i>	<i>R. chunii</i>	<i>Rhizosolenia</i> spp.	<i>Thalassiosira lentiginosa</i>	<i>Thalassiosira oliverana</i>	<i>T. tumida</i>	<i>Thalassiothrix antarctica</i>	
A1	ZN-007	25	m	c	c	c	c	c	c	m	c	c	m						r	d	
A3a	ZN-001	17	m		c	r	c	c	c		m/c		c							d	
A3b	ZN-006	29	m/c	c	c	r	m	c	c	c	c	c	m	r/m	r				r	d	
A3c	ZN-008	22	m	m	c	c	m	c	c	c/m	m		m					r/m		d	
A3d	ZN-010	26	m	r	c	m	m	c	c	r	m		m					m		d	
A3e	ZN-023	28	r/m	r	c/d	m	m	m/c	m	c	m/c		m/c				r			c	
A3f	ZN-033	26	m/c	c/d	r/m	c	c	r	m	m/c	r		r				m/c			m	
A3g	ZN-034	22	r/m	c/d	m	r/m	m	m	m	m/c			c/d				r/m			m	
A5	ZN-005	24	m	m/c	c	r	r	c	m	m	c		c					r/m		d	
A7	ZN-004	22	r	m	c		c	c	m	m	c		m	m/c	r			r		d	
A9	ZN-003	18	m	m	c		r	c	c	m	c		c							d	
A11	ZN-002	16	r	m	m	m	c	c	c		m		c							d	
B01	ZN-021	25	m	r	m	r	m	c	c/d	r	m		m							c/d	
B03	ZN-020	31	m	m	m	m	c/m	c/d	c	r	m		m	r			m/c			c/d	
B05	ZN-019	21	m	c	m	m	c	d	d		m/c		r							d	
B07	ZN-018	28	c	c	r		c/d	r	c/d		m		m							c/d	
B9	ZN-017	22	c	c			c	c	c	r	m		m							d	
B11	ZN-016	23	c				c	d	d		m		m							c	
C01	ZN-030	27	c	m/c	c	r	c	r	m		r	d	m							c	m
C03	ZN-029	22	c	m	m/c		c	r	m/c		r	c	c						m/c	d	
C05	ZN-027	24	c	m	m		c/d		m/c		r/m		r						m/c	c/d	
C07	ZN-026	24	m/c	r	m/c	r	c	r	m		r/m		r						m	d	
C09	ZN-025	24	m/c	r	m/c	r	c		c		m/c		r						m/c	d	
C11a	ZN-011	20	m	r	m	m	m	m	c		m		r							d	
C11b	ZN-012	28	r	r	r/m	m	m	r/m	m/c	r	m		r						r	d	
C11c	ZN-013	32	c	m	c		c	r/m	d		r/m		m							c	
C11d	ZN-014	26	m	r	m/c		m/c	r	d		m		r							d	
C11e	ZN-024	26	m/c	r	r/m		c	r/m	c		m/c		r						m/c	d	

r: rare, m: minor, c: common, d: dominant.

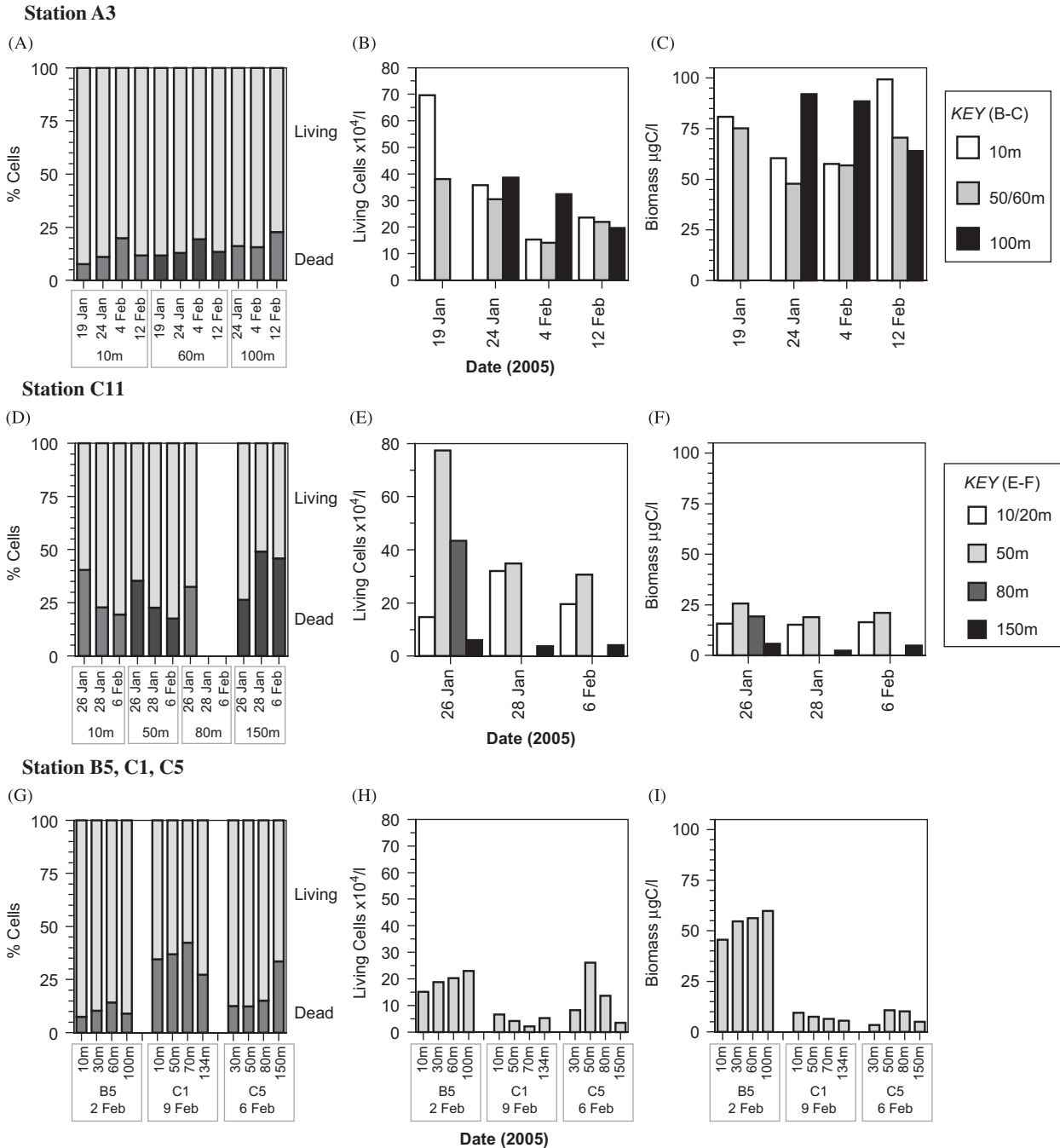


Fig. 3. Summary of cell and biomass contributions at stations A3, C11, B5, C1 and C5: (A, D and G) percentage dead and living cells by date and depth per station, (B, E and H) living cells $\times 10^4 L^{-1}$ by date and depth per station, and (C, F and I) calculated biomass $\mu g C L^{-1}$ by date and depth.

to A3 was due to a thanatocoenose composed of both atypic and typic *E. antarctica* cells (6%) and *Chaetoceros* resting spores (11%).

Focussing on the A3 living assemblage (Fig. 3B), the largest concentration was observed in the surface waters at the start of the survey (69×10^4 cells L^{-1}), which decreased to around 21×10^4 cells L^{-1} by the end. The small *Chaetoceros Hyalochaete* group accounted for 74% of the initial surface assemblage, with *Thalassionema nitz. f. nitzschoides* and *F. kerguelensis* contributing approxi-

mately 3% and 2%, respectively (Table 5). This surface dominance of *Chaetoceros Hyalochaete* spp. decreased at 50m depth to 52%, against the increase of *E. antarctica* (typic), *Navicula* spp. and *F. kerguelensis* (Table 5). The trade off in numbers between depths and major species at the start of the survey (19 January) was observed in the total biomass conversion (Figs. 3C and 4), whereby the decrease in the small *Chaetoceros Hyalochaete* spp. biomass was offset by the large and intermediate biomass contributing cells of *T. antarctica* and *E. antarctica* (typic).

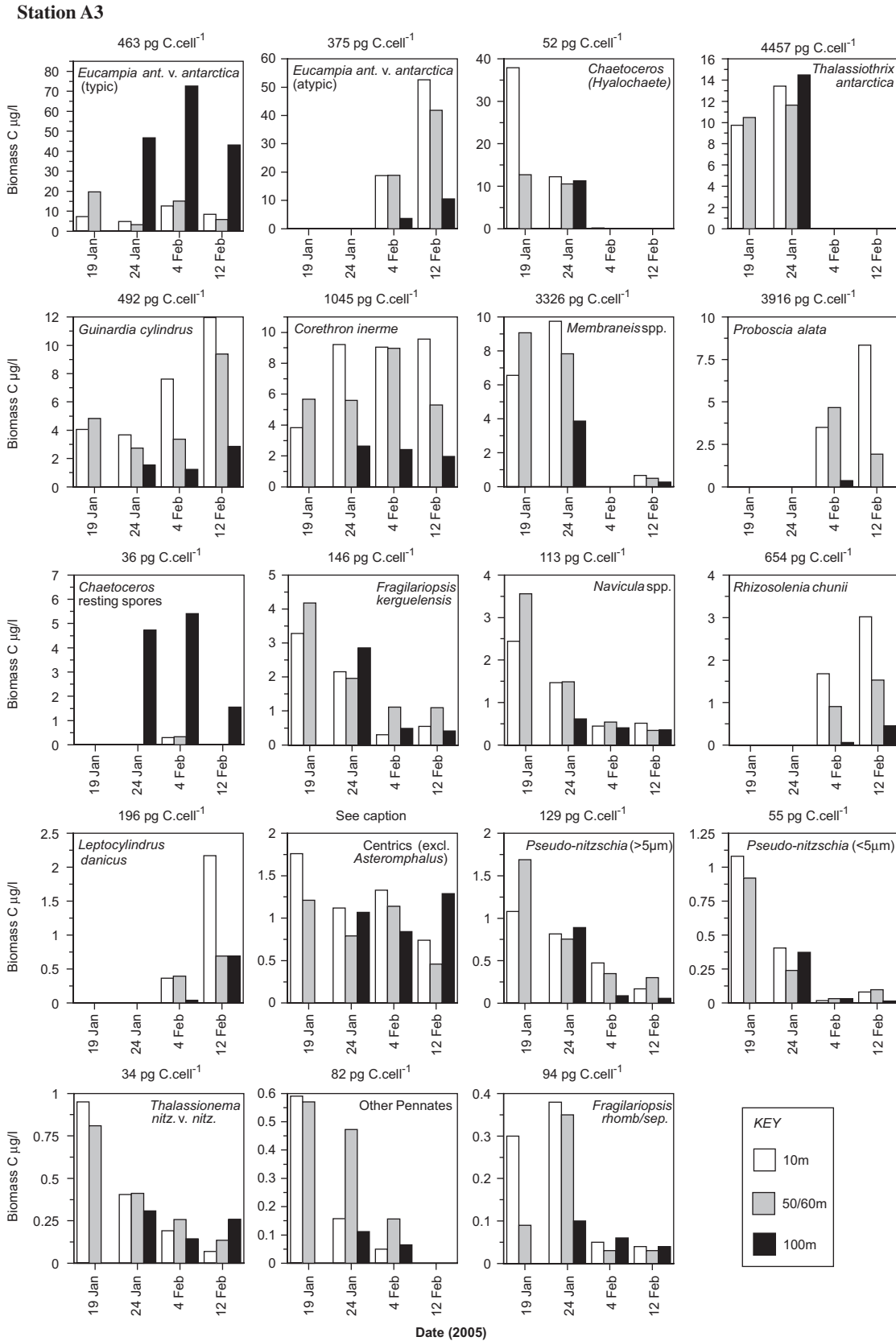


Fig. 4. A3 major diatom biomass contributions. Carbon biomass contribution by species, depth and date at Station A3. The average cell carbon content per species (incorporating changes in size across the whole survey period) is given above each plot. The 19 January mid-water sample was taken at 50m depth and at 60m on other dates. Species notes: *Eucampia ant. v. ant.* (typic = normal chains and vegetative cells; atypic = abnormal cells) *Pseudo-nitzschia* spp. (<5µm and >5µm transapical width delineation). Centrics (excluding observations of *Asteromphalus* spp.). Centric biomass values are a summation of the following species (mean biomass per cell listed here): *A. tabularis* = 4812pg C cell⁻¹, *T. gracilis* 70 pg C cell⁻¹, *T. lentiginosa*, 1246 pg C cell⁻¹, *Thalassiosira* spp. = 904 pg C cell⁻¹ taken from C11 values, Other Centrics = 746 pg C cell⁻¹.

Table 4
Total and integrated biomass results from CTD stations

Station	Date	Depth (m)	Total biomass ($\mu\text{g C L}^{-1}$)	Mixed layer depth (m) ^a	Integrated biomass over MLD (mg C m^{-2}) ^b	Av. cell abundance $\times 10^4 \text{ L}^{-1}$ ($10 \leq 80 \text{ m}$) ^c
A3-1	19/1/05	10	80.8	52.3	3935	53.9
A3-1		50	75.2			
A3-3	24/1/05	10	60.3	50.8	2560	33.1
A3-3		60	47.8			
A3-3		100	92.1			
A3-4	4/2/05	10	57.5	78.5	5369	14.8
A3-4		60	56.8			
A3-4		100	88.4			
A3-5	12/2/05	10	99.4	83.9	5588	22.8
A3-5		60	70.5			
A3-5		100	63.9			
B5	2/2/05	10	45.6	83.6	4875	18.0
B5		30	54.6			
B5		60	56.2			
B5		100	59.8			
C1	9/2/05	10	9.6	128.5	708	4.3
C1		50	7.5			
C1		70	6.5			
C1		134	5.5			
C5	8/2/05	30	3.4	80	824	16.0
C5		50	10.7			
C5		80	10.3			
C5		150	5.0			
C11-1	26/1/05	20	15.8	77.7	1554	45.0
C11-1		50	25.7			
C11-1		80	19.3			
C11-1		150	5.8			
C11-2	28/1/05	10	15.1	78.3	1119	33.5
C11-2		50	18.9			
C11-2		80				
C11-2		150	2.5			
C11-3	6/2/05	10	16.4	56	1137	25.1
C11-3		50	21.0			
C11-3		80				
C11-3		150	4.9			

^aMixed layer depth data (MLD) is sourced from the KEOPS shipboard data.

^bIntegrated biomass values were calculated from the samples within the mixed layer.

^cThe cell abundance in the surface waters for each station/visit is an average of values encountered at depths between 10 and 80 m dependent on sample availability.

The second visit repeated the dominating cellular abundance of *Chaetoceros Hyalochaete* spp., *Navicula* spp., *T. nitz. f. nitzschoides* and *F. kerguelensis* in the 10 and 60 m layers. At 100 m depth *Chaetoceros Hyalochaete* spp. abundances decreased, but the taxa remained the most abundant group, regardless of the large increases in *Chaetoceros* resting spores and *E. antarctica* typic cells (Table 5).

The number of cells per litre on the third visit (4 February, Fig. 3B) was dramatically diminished in the surface layers and represented a major change in the diatom community; dominated by *E. antarctica* at 10 and 50 m (av. 30% atypic and 17% typic cells, Table 5). At 100 m depth the assemblage was dominated exclusively by typic *E. antarctica* cells (45%) and *Chaetoceros* resting spores (30%) (Table 5 and Fig. 4). At the end of the survey

(12 February) the cell concentrations varied little with depth (between $20\text{--}25 \times 10^4 \text{ cells L}^{-1}$). In contrast to the third visit assemblage, the surface water abundances during the final visit increased due to a build up of three large cylindrical species (*P. alata*, *G. cylindrus*, and *R. chunii*), the small *Leptocylindrus danicus* and the most abundant species, atypic *E. antarctica* (Appendix 3). *Chaetoceros* resting spores and normal *E. antarctica* cells again dominated the 100 m sample (Table 5).

The conversion of these cell abundances to biomass (via volume), changes the structure of assemblage composition and dominance. Thus, although the number of cells in the waters at Station A3 decreased over time the contribution to biomass in fact marginally increased dependent on depth (Fig. 3B and C). In essence this was due to the replacement of the small and numerous *Chaetoceros Hyalochaete* spp.

Table 5
Major species abundances at Station A3^a

Date	Depth (m)	<i>Chaetoceros Hyalochaete</i> spp.	<i>Chaetoceros</i> resting spores	<i>Eucampia antarctica</i> (atypic)	<i>Eucampia antarctica</i> (typic)	<i>Fragilariopsis kerguelensis</i>	<i>Guinardia cylindrus</i>	<i>Navicula</i> spp.	<i>Pseudo-nitzschia</i> spp. (< 5 µm)	<i>Thalassionema nitz. f. nitz.</i>
19-Jan	10	57.3 ^b (74 ^c)	0.03 (0.04)	0.01 (0.01)	1.6 (2.1)	1.9 (2.4)	0.8 (1.1)	1.7 (2.2)	1.4 (1.9)	2.5 (3.2)
	50	23.4 (51.8)	–	0.7 (0.3)	3.2 (7.2)	2.1 (4.7)	0.8 (1.6)	2.6 (5.7)	1.4 (3.1)	1.7 (3.9)
24-Jan	10	26 (63)	0.1 (0.2)	0.5 (0.1)	0.5 (1.2)	1.3 (3.2)	0.7 (1.7)	1.6 (4)	0.7 (1.7)	1.4 (3.4)
	60	21 (58)	0.1 (0.3)	0.1 (0.3)	0.7 (1.9)	1.39 (3.9)	0.6 (1.8)	1.6 (4.5)	0.6 (1.5)	1.39 (3.9)
	100	22 (33.7)	14.8 (22.9)	0.01 (0.02)	10.2 (15.8)	1.8 (2.8)	0.3 (0.5)	0.7 (1.0)	0.8 (1.3)	1 (1.6)
4-Feb	10	0.3 (1.5)	0.6 (3.3)	5.8 (31.8)	3.1 (15.6)	0.2 (1.1)	1.4 (7.2)	0.4 (1.8)	0.05 (0.3)	0.7 (3.3)
	60	0.1 (0.4)	0.7 (4.1)	5.1 (28.7)	3.2 (18.3)	0.6 (3.5)	0.8 (4.5)	0.5 (2.7)	0.05 (0.3)	0.9 (4.9)
	100	0.1 (0.2)	11.8 (30)	1 (1.4)	17.5 (44.5)	0.3 (0.8)	0.3 (0.6)	0.3 (0.8)	0.07 (0.2)	0.5 (1.2)
12-Feb	10	0.01 (0.04)	0.1 (0.2)	15 (54.8)	1.4 (5.2)	0.4 (1.6)	2.6 (9.4)	0.4 (1.6)	0.2 (0.8)	0.4 (1.4)
	60	0.04 (0.2)	0.01 (0.04)	15.2 (59)	1.3 (5)	0.7 (2.8)	2.1 (8)	0.4 (1.5)	0.2 (0.6)	0.4 (1.6)
	100	–	5.3 (20.6)	3.2 (12.3)	8.6 (33.1)	0.3 (1)	0.6 (2.1)	0.3 (1)	0.02 (0.1)	0.8 (2.9)

^aThis data is a subset of Appendix 3.

^bCell abundance $\times 10^4$ cells per litre.

^cBracketed value = percentage contribution to the complete diatom assemblage encountered (living and dead cells inclusive).

(from a surface average of 36.6–0.1 µg CL⁻¹) with a larger sized *E. antarctica* assemblage (from a surface av. of 17.6–87.1 µg CL⁻¹) between the first two and last two visits. We noted above that there was an abrupt shift in species composition during the first visit from a diatom community dominated by *Chaetoceros Hyalochaete* spp. at 10 m to one dominated by *E. antarctica* (typic) at 60 m depth. In terms of biomass, this shift was marked by increased biomass contributions of *E. antarctica* and *T. antarctica* (Fig. 4). At the second visit (Fig. 3C), the large increase in biomass at 100 m was attributable to the following species: *E. antarctica* (typic, 46.8 µg CL⁻¹), *T. antarctica* (14.5 µg CL⁻¹), *Chaetoceros Hyalochaete* spp. (11.3 µg CL⁻¹), *Chaetoceros* resting spores (4.7 µg CL⁻¹), *Membraneis* spp. (3.9 µg CL⁻¹), *F. kerguelensis* (2.9 µg CL⁻¹) and *C. inerme* (2.6 µg CL⁻¹) (Fig. 4). Some of these species occurred in low cell numbers in the samples; however, due to their large size, they contributed substantially to the biomass total. The surface sample biomass total (10–60 m) was dominated in both cases by three large-sized diatom species (*T. antarctica*, *Membraneis* spp. and *Corethron inerme*), followed by small-sized but numerous *Chaetoceros Hyalochaete* spp. *Membraneis* spp. were also undergoing division during the first two sampling dates, enhancing their population size and thus biomass. At the third visit (4 February) the diatom assemblage composition changed radically from the previous samples. We observed large biomass decreases in the small *Chaetoceros Hyalochaete* spp., *Membraneis* spp., *F. kerguelensis*, *Navicula* spp., both *Pseudo-nitzschia* spp., *Thalassionema nitz. f. nitzschiioides* and various pennate spp. (Fig. 4). However, this decrease was compensated by a concomitant increase in large cylindrical diatoms (e.g. *Corethron inerme*, *G. cylindrus* and *P. alata*) and the sustained dominance of typic *E. antarctica* cells (no longer

in coiling chains) and *Chaetoceros* resting spores at 100 m depth explaining the rather stable total biomass between visits 2 and 3 (Fig. 3C).

At the last visit (12 February) the peak in surface biomass at 10 m (Fig. 3C) was mainly due to atypic *E. antarctica* (52.6 µg CL⁻¹), *G. cylindrus* (12.0 µg CL⁻¹), *C. inerme* (9.6 µg CL⁻¹), typic *E. antarctica* (8.4 µg CL⁻¹), *P. alata* (8.3 µg CL⁻¹), *R. chunii* (3.0 µg CL⁻¹) and *L. danicus* (2.2 µg CL⁻¹) (Fig. 4). The drop in biomass at 100 m depth from the 4 to 12 February was the result of decreases in *Chaetoceros* resting spores and *E. antarctica* (typic), but included an offset by *G. cylindrus* and *T. lentiginosa* cells (Appendix 3, the latter species are shown in Fig. 4 as an increase in the plot “Centrics” at 100 m).

The average cell biomass contribution averaged over depth and date for each species is given above each species plot in Fig. 4 (a complete list of individual biomass values per species and date are found in Appendix 4—Supplementary Material). Of the major total biomass contributors at station A3, six are considered small biomass contributors, nine as intermediate and eight as large. The largest total biomass contributor at A3 was the intermediate-sized *E. antarctica* (all types).

In general, the average size of more than half of the species observed (e.g., *Chaetoceros Hyalochaete* spp., *E. antarctica* typic, *F. kerguelensis*, *G. cylindrus*, *P. alata*, *Odontella weissflogii*, *Haslea trompii*, *Pseudo-nitzschia* and *Membraneis* spp.) taken over all the depths for any one date were larger when sampled at the first visit (19 January) (Appendix 4—Supplementary Material). Species such as *Membraneis* (average volume at 10 m: 101,992 µm³, at 50 m: 200,877 µm³) and *E. antarctica* (typic) (average volume at 10 m: 8860 µm³, at 50 m 13,3326 µm³) were larger at 50 m depth than in the surface sample.

3.2.2. Station C11

Station C11, located off-plateau in the HNLC region, revealed a larger percentage of dead and empty cells ranging between 17.6% and 49% over the upper 150 m (Fig. 3D). The thanatocoenose assemblage accounted for nearly 50% of the total diatom assemblage at the last two station visits. The first visit (26 January) revealed an elevated thanatocoenose abundance in the surface waters above 150 m. The major contributors at 10 m, where 40% of the assemblage was dead, were the minute pennate *Fragilariopsis pseudonana* (30%) and *F. kerguelensis* (4%). At the second visit (28 January) the thanatocoenose of the surface waters comprised 20% of the total diatom assemblage and increased to 49% at 150 m depth. This large contribution was reflected by a 24% relative abundance of *F. kerguelensis* (against a 7% biocoenose contribution), a 5% contribution from the *Fragilariopsis separanda/rhombica* group and an 8% contribution from *F. pseudonana*. At the last visit (6 February), surface contributions of non-living material diminished to ~18%, but remained elevated at 150 m depth with 46% of the total diatom assemblage allocated as dead cells. Again *F. kerguelensis*, *F. pseudonana* and *F. separanda/rhombica* played major roles in this thanatocoenose with 19%, 9% and 3%, respective contributions. *Pseudo-nitzschia* spp. (<5 µm) and “Other Centrics” also contributed 3% equally to this total thanatocoenose percentage.

The total abundance of the living assemblage generally remained between 10×10^4 and 40×10^4 cells L^{-1} in surface waters (10–80 m) (Fig. 3E). The exception being at 50 m, during the first visit, where 78×10^4 cells L^{-1} were encountered. In this instance 56% were contributed by *F. pseudonana* (Table 6). At 80 m depth *F. pseudonana* continued to contribute around half of the observed cellular count in the living fraction (Table 6). In both cases this species far outweighed any other species in terms of abundance by a factor of at least 11–13 times to the next

abundant species *F. kerguelensis*. *Cylindrotheca closterium* was generally the third most abundant species but was poorly represented at 2–6% of the total assemblage over 10–80 m depth. The 150-m depth samples clearly indicated a drastic reduction in living cell contributions (Table 6 and Fig. 3E). All species were still present as live cells at this depth, albeit at low abundances. *Fragilariopsis kerguelensis*, *F. pseudonana* and *C. closterium* represented the “most abundant” taxa at this depth.

Biomass contributions at C11 as a total and by species are presented in Figs. 3F and 5, respectively. The average cell biomass contribution averaged over depth and date for each species is given above each plot in Fig. 5 (Appendix 4). Of the total biomass contributors at C11, seven were considered small biomass contributors, six as intermediate and ten as large. Similar to station A3 the numerically dominant taxa did not control the carbon budget. Total biomass over the survey period at C11 remained relatively constant with respect to depth, varying between 15 and $25 \mu g CL^{-1}$ at and above 80 m depth and between 2 and $5 \mu g CL^{-1}$ at 150 m (Fig. 3F). The largest biomass contributors in decreasing order were *F. kerguelensis* (intermediate biomass species), *T. lentiginosa* (large), *T. antarctica* (large), *F. pseudonana* (small) and *F. separanda/rhombica* (intermediate) (Fig. 5). The biomass contribution of *F. kerguelensis* declined over the course of the survey at all depths (i.e. *F. kerguelensis*' total biomass decreased from $21.8 \mu g CL^{-1}$ on 26 January to $6.97 \mu g CL^{-1}$ on 6 February, Fig. 5). Its biomass was principally replaced by the increased contributions from *T. lentiginosa* and *T. antarctica*, both large biomass contributing species. By the last visit to C11, centrics were the greatest biomass contributors at all depths (10–50 m = $8\text{--}10 \mu g CL^{-1}$, 150 m = $3 \mu g CL^{-1}$). At 150 m the living diatom community was low in numbers and the biomass rather equally distributed over all species. With the exception of four species (*F. kerguelensis*, *T. lentiginosa*, “Other Centrics” combined and *T. antarctica*, Fig. 5), the

Table 6
Major species abundances at Station C11^a

Date	Depth (m)	<i>Cylindrotheca closterium</i>	<i>Fragilariopsis kerguelensis</i>	<i>Fragilariopsis pseudonana</i>	<i>Fragilariopsis separanda / rhombica</i>	<i>Pseudo-nitzschia</i> spp. (<5 µm)	Other Centrics	Other Pennates
26-Jan	20	1 ^b (4 ^c)	5.7 (23)	3.7 (15)	0.4 (1.7)	0.3 (1.3)	0.4 (1.8)	1.4 (6)
	50	2.4 (2)	5.1 (4)	67.3 (56)	0.2 (0.1)	0.2 (0.1)	0.7 (0.6)	0.8 (0.7)
	80	1.4 (2)	3.8 (6)	34.6 (53)	0.6 (0.9)	0.7 (1)	0.8 (1)	0.7 (1)
	150	1.1 (13)	1.7 (20)	1.7 (20)	0.1 (1.6)	0.5 (6)	0.2 (2)	0.1 (1.2)
28-Jan	10	2.2 (5)	3.4 (8)	22.9 (54)	0.9 (2)	0.5 (1.3)	0.7 (1.5)	0.9 (2)
	50	2.4 (5)	3.8 (8)	24.8 (54)	1.6 (3)	0.5 (1)	0.8 (1.7)	0.5 (1.1)
	150	0.4 (4.1)	0.6 (6.6)	1.9 (21.9)	0.3 (3.3)	0.5 (5.1)	0.1 (1.3)	0.01 (0.1)
5-Feb	10	1.0 (4)	1.2 (5)	15.4 (63)	0.4 (1.7)	0.3 (1.1)	0.5 (2)	0.5 (1.9)
	50	1.8 (4.7)	2.8 (7.4)	23.4 (63)	0.9 (2.5)	0.2 (0.6)	0.5 (1.3)	0.6 (1.5)
	150	0.9 (11)	0.6 (7.2)	2.1 (26)	0.02 (0.3)	0.2 (2.5)	0.1 (1.5)	0.1 (1.5)

^aThis data is a subset of Appendix 3.

^bCell abundance in $\times 10^4$ cells per litre.

^cBracketed value = percentage contribution to the complete diatom assemblage encountered (living and dead cells inclusive).

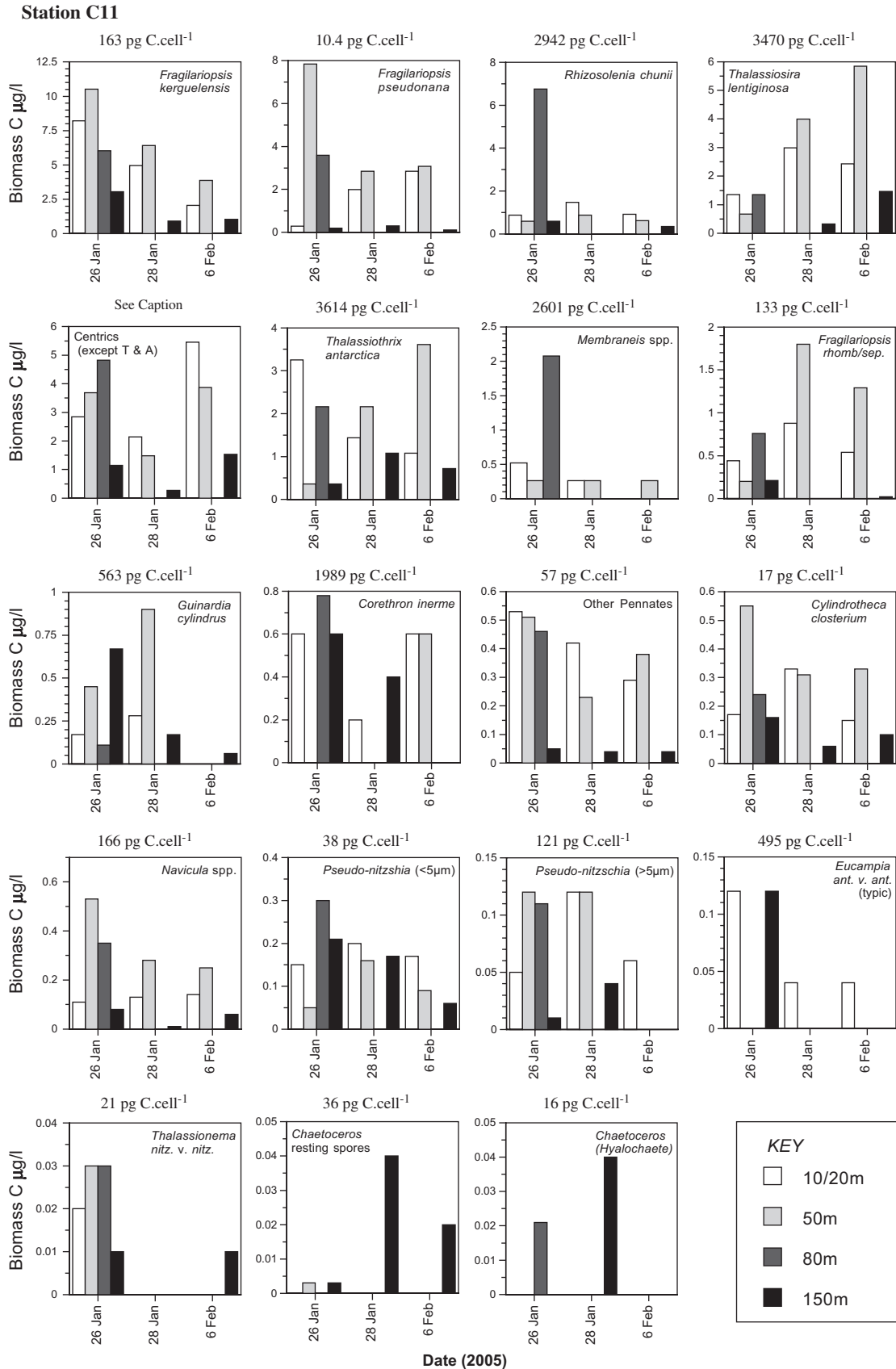


Fig. 5. C11 major diatom biomass contributions. Carbon biomass contribution by species, depth and date at Station C11. The average cell carbon content per species (incorporating changes in size across the whole survey period) is given above each plot. Notes: The 26 January surface sample was taken at 20m depth and at 10m on other dates. *Pseudo-nitzschia* spp. (<5µm and >5µm transapical width delineation). Centrics (excluding observations of *Thalassiosira lentiginosa* and *Asteromphalus* spp.). Centric biomass values are a summation of the following species (mean biomass per cell listed here): *A. tabularis* = 1516 pg C cell⁻¹, *T. gracilis* = 101 pg C cell⁻¹, *T. lentiginosa* = 3470 pg C cell⁻¹, *Thalassiosira* spp. = 904 pg C cell⁻¹, and other centrics = 259 pg C cell⁻¹.

Stations B5, C1 and C5

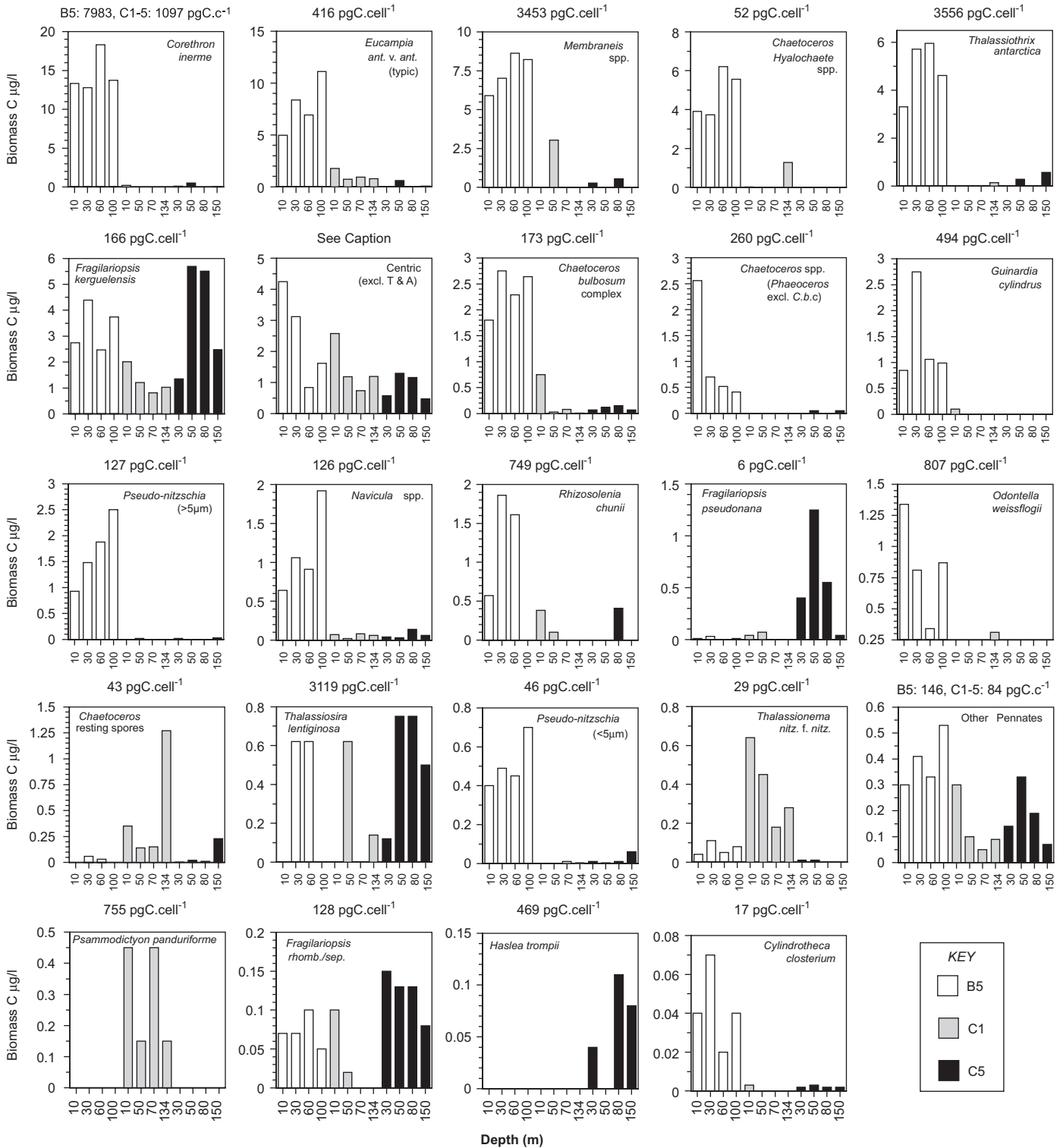


Fig. 6. Stations B5, C1 and C5 major diatom biomass contributions. Carbon biomass contribution by species and depth at Station B5, C1 and C5 in approximate order from largest to smallest biomass contributors. Notes: Sample dates; B5 = 2/2/05, C1 9/2/05, C5 = 6/2/05. *Pseudo-nitzschia* spp. (<5µm and >5µm transapical width delineation), *Chaetoceros* spp. (*Phaeoceros* excluding *C. bulbosum* complex), Centrics (excluding observations of *Thalassiosira lentiginosa* and *Asteromphalus* spp.). An average biomass contribution per species value over all three stations is given above each plot, with exception to where a difference in sizes was noted. Centric biomass values are a summation of the following species (mean biomass per cell listed here): *A. tabularis* = 1803 pg C cell⁻¹, *T. gracilis* = 109 pg C cell⁻¹, *Thalassiosira* spp. = 904 pg C cell⁻¹ taken from C11 values, other centrics = 372 pg C cell⁻¹.

remaining diverse assemblage contributed no more than $1 \mu\text{g CL}^{-1}$ per species. The exceptions contributed at different times biomass up to $\sim 3 \mu\text{g CL}^{-1}$.

In terms of community structure we did not observe the abrupt change from one community to another over the late January/early February period at C11 in contrast to Station A3. Nonetheless, there was evidence for a small shift in the community to larger biomass species as mentioned above. In parallel, the size of *F. kerguelensis* was larger at the first visit than at the last (26 January: average apical axis $41 \mu\text{m}$ – $180 \mu\text{g CL}^{-1}$; 6 February: $35.3 \mu\text{m}$ – $158 \mu\text{g CL}^{-1}$), whereas for *Thalassiosira lentiginosa*, size increased over time (26 January: average diameter $41.5 \mu\text{m}$ – $1347 \mu\text{g CL}^{-1}$; 6 February: $72.8 \mu\text{m}$ – $4864 \mu\text{g CL}^{-1}$). Other species, such as *Pseudo-nitzschia* spp. ($> 5 \mu\text{m}$), *Thalassionema nitz. f. nitzschoides*, *G. cylindrus* and *Membraneis* spp., were absent or reduced in presence at the last survey visit to C11 (Fig. 5).

3.2.3. Station B5

The three remaining stations were sampled during early February on single occasions during the KEOPS mission. Station B5 revealed the lowest contribution of non-living cells of the KEOPS study (average 10.3%, Appendix 3, Fig. 3G). The greatest number of dead species was observed at 60 m depth, where the contribution of *Pseudo-nitzschia* spp. (5%), *F. kerguelensis* (2.1%), *Navicula* spp. (1.1%) and *C. inerme* (1%) dominated the thanatocoenose. Living cell contributions of this diverse community increased with depth, varying between $15 \times 10^4 \text{ cells L}^{-1}$ at 10 m and $23 \times 10^4 \text{ cells L}^{-1}$ at 100 m (Fig. 3H, Appendix 3). As a function of species composition the major contributors over all depths studied were: *Chaetoceros Hyalochaete* spp. averaging 34–53% relative abundance (6.9 – $11.5 \times 10^4 \text{ cells L}^{-1}$), *F. kerguelensis* 7–13% (1.5 – $2.7 \times 10^4 \text{ cells L}^{-1}$), *C. bulbosum* complex 7–10% (1 – $1.6 \times 10^4 \text{ cells L}^{-1}$), *E. antarctica* typic cells 6–9% (1.0 – $2.3 \times 10^4 \text{ cells L}^{-1}$) and *Pseudo-nitzschia* spp. ($> 5 \mu\text{m}$) with 5–8% (0.7 – $2 \times 10^4 \text{ cells L}^{-1}$). *Chaetoceros Hyalochaete* spp. clearly increased in abundance at 60 and 100 m compared to surface observations.

Station B5 Biomass total was large, coming second to Station A3. In contrast to A3, biomass contributions at Station B5 increased with depth but ranged closely from 45.6 to $59.8 \mu\text{g CL}^{-1}$ over 90 m (Fig. 3I). The major contributor of biomass was the large-sized *C. inerme* community (Fig. 6, Appendix 4). This species played a minor role in cell abundance ($< 1\%$) but accounted for 22–31% of the carbon biomass, due to its average $7983 \text{ pg C cell}^{-1}$ contribution, the largest observed by any diatom species in the entire KEOPS study. Other species contributing to the high biomass totals included the *E. antarctica* typic (intermediate biomass species contributor, average 12% total biomass contribution over depth), *Membraneis* spp. (large, average 14%), *T. antarctica* (large, average 9%), *Chaetoceros Hyalochaete* spp. (small, average 8%), *F. kerguelensis* (intermediate, average 6%) and

P. alata (large, average 4%). Station B5 was represented in general by six small, ten intermediate and ten large diatom biomass contributing species. The major species departure at Station B5 from all other stations was the presence and diversity in the *C. bulbosum* complex. We recognised three types: the typical *Chaetoceros atlanticus* Cleve, the small and rectangular *C. atlanticus* var. *neapolitana* (Schroder) Hustedt, and the single, inflated setae (horned) cell, identified in the literature as the *bulbosum* phase. These variations were observed at 2.8 , 2.5 and $0.04 \times 10^4 \text{ cells L}^{-1}$ and contributed 7.3 , 2.2 and $0.1 \mu\text{g CL}^{-1}$, respectively, depth integrated.

3.2.4. Station C1

Station C1 in the vicinity of Heard Island (Fig. 1) contained a large thanatocoenose in the surface waters representing by 35–42% of the total, decreasing to 27% at 134 m (Fig. 3G, Appendix 3). Species contributing to this assemblage included *F. kerguelensis* (13%), *E. antarctica* typic (2%), *Thalassionema nitz. f. nitzschoides* (8%) and other Pennates (3%). Cell abundance presented in Fig. 3H, was the lowest encountered ranging from 2 to $6.9 \times 10^4 \text{ cells L}^{-1}$. The living assemblages at 10 and 50 m were similar, both dominated by *Thalassionema nitz. f. nitzschoides* (32–38%, 1.6 – $2.2 \times 10^4 \text{ cells L}^{-1}$), very short chains of *F. kerguelensis* (19%, 0.8 – $1.3 \times 10^4 \text{ cells L}^{-1}$), *Chaetoceros* resting spores (8–11%, 0.3 – $0.8 \times 10^4 \text{ cells L}^{-1}$) and *F. pseudonana* (7–16%, 4.5 – $6.6 \times 10^4 \text{ cells L}^{-1}$). At 70 m, there was a loss of *F. pseudonana* and *F. sep./rhombica* cells. Dominant species remained in order of greatest impact, *Thalassionema nitz. f. nitzschoides*, *F. kerguelensis*, and *Chaetoceros* resting spores, but the abundance of *E. antarctica* typic cells increased to 10%, placing it as the 4 important species. At 134 m depth *Chaetoceros* resting spores increased to 55% ($2.9 \times 10^4 \text{ cells L}^{-1}$), with the other remaining abundant species following in order as at 70 m, albeit at lower abundances.

Biomass was low at Station C1 ranging between 5.5 and $9.6 \mu\text{g CL}^{-1}$, with dominant contributions from *F. kerguelensis* (20% total contribution of biomass) and *E. antarctica* (18%) in the surface waters (10–50 m), but at depth no single species dominated (Fig. 6). Station C1 represented a poor community with respect to the diversity and abundance observed at the other stations. Nevertheless, one benthic species was unique to this station alone: *Psammodyctyon panduriforme* (synonym *Nitzschia panduriformis*, Round et al., 1990). It was observed at less than 1% at all depths sampled and supplied 3–4% of the total biomass. No other benthic species were observed.

3.2.5. Station C5

Station C5 located in the northeastward trending bathymetric channel over the plateau was sampled on the 6 February. The diatom assemblage was represented by a low proportion of dead cells in the surface waters (12–15%), which increased to 33% at 150 m (Fig. 3G).

The thanatocoenose was dominated by pennates, most notably *F. pseudonana* (average 7%), *F. kerguelensis* (average 4%) and *F. rhombica/separanda* (average 0.8%). At 150 m *F. kerguelensis* dominated the thanatocoenose outright at 19% (Appendix 3). The living assemblage in terms of cells per litre (Fig. 3H) revealed a large increase at 50 m in comparison to the 30 m “surface” sample ($8.2\text{--}26.1 \times 10^4 \text{ cells L}^{-1}$). This peak was due almost entirely to increases in *F. pseudonana* ($6.78\text{--}21.58 \times 10^4 \text{ cells L}^{-1}$) and *F. kerguelensis* ($0.76\text{--}3.21 \times 10^4 \text{ cells L}^{-1}$), although centric species played an important role in the abundances at this depth. The subsequent decrease in cell numbers at 80 m corresponded to the drop in *F. pseudonana* abundance to $9.5 \times 10^4 \text{ cells L}^{-1}$. *Fragilariopsis kerguelensis* abundance remained similar to the abundance at 50 m. The sole appearance of *R. chunii* and the highest abundance of *Haslea trompii*, a large pennate, occurred at this depth and location.

The living assemblage at 150 m was very poor and low in abundance ($35 \times 10^3 \text{ cells L}^{-1}$). *Fragilariopsis kerguelensis* replaced *F. pseudonana* as the dominant species, the latter, which in turn was almost absent at this depth in contrast to previous depths ($5.2 \times 10^3 \text{ cells L}^{-1}$). *Chaetoceros* resting spores ($7.9 \times 10^3 \text{ cells L}^{-1}$), *Pseudo-nitzschia* spp. ($< 5 \mu\text{m}$) ($1.4 \times 10^3 \text{ cells L}^{-1}$) both increased in dominance at 150 m even though their numbers were low.

Station C5, like Station C1, had low biomass contributions ranging from 3.4 to $10.7 \mu\text{g CL}^{-1}$ (Fig. 3I, Appendix 4). “Surface” values of $3.39 \mu\text{g CL}^{-1}$, were mainly composed of *F. kerguelensis* ($1.35 \mu\text{g CL}^{-1}$), a combination of all other centrics ($0.63 \mu\text{g CL}^{-1}$) and *F. pseudonana* ($0.4 \mu\text{g CL}^{-1}$) (Fig. 6). Regardless of the large abundance of *F. pseudonana* at 50 m depth (total biomass equal at 50 and 80 m), *F. kerguelensis* continued to be the major dominant supplier of carbon (5.7 and $5.5 \mu\text{g CL}^{-1}$, respectively, $> 50\%$ of the total biomass), with all the centrics combined coming second (2.04 and $1.9 \mu\text{g CL}^{-1}$, respectively). At 150 m the total biomass of all species decreased to $5.4 \mu\text{g CL}^{-1}$. The only change to the individual species biomass contributions were a loss of *F. pseudonana* and a minor increase in *Chaetoceros* resting spores. *Fragilariopsis kerguelensis* remained the major biomass contributor.

Finally, Station C5 although similar in biomass contribution to Station C1, did not show the same fragmented assemblage. The species assemblage was in fact much closer to that observed at Station C11 off-plateau, although the size of certain species, such as *F. pseudonana* and *R. chunii* remained small compared to observations of the same species at C11 (Appendix 4).

4. Community assessment

4.1. Net and CTD variations

Comparison between the net hauled material and CTD analysis revealed a loss of information in the CTD samples,

as previously noted by Kopczyńska et al. (1986). In general though, changes in the species community agreed between the net hauls and CTD assessment. This was most clearly seen with the change in community composition at Station A3 with the loss of *T. antarctica* as the dominant constituent being replaced by *P. alata* and *C. inerme* in later net hauls. A similar trend also was observed under the CTD sampling at A3. The role of *D. antarcticus* proved troublesome, it was abundant in net hauls but was often difficult to find complete in CTD samples. In contrast, the surface assemblage defined by net hauls at C1 near Heard Island was dominated by either large centrics (*Thalassiosira lentiginosa*, *T. tumida* and *Asteromphalus hookerii*) or large cylinder shaped taxa (*Rhizosolenia* spp. *D. antarcticus* and *Corethron inerme*) none of which made any large impact on the abundance or biomass reported from the CTD sample.

In general, the larger taxa dominant in the net hauls was not captured by the CTD sampling. Settling within Niskin bottles and small sub-sample size from the Niskins may have resulted in the discrepancies observed between the two sampling protocols. The net technology also has limitations of course, including varying depth control, changes in mesh size and variable clogging due to large or needle-shaped species abundance in certain regions. This continuing methodological discrepancy between net and CTD analyses represents a limitation to diatom biomass estimates undertaken by the latter method; a point that Kemp et al. (2006) highlighted as a future challenge in sampling larger diatoms and their true contribution to the Si and C cycles. A solution may be to use in-situ pump filtering or phytoplankton-adapted rectangular mid-water trawls (RMTs). The remainder of our discussion focuses on the CTD results.

4.2. Geographic patterns

On the plateau, stations A3 and B5 were the most similar in terms of the species and high biomass encountered. These stations representative of bloom conditions had elevated abundances of *Chaetoceros Hyalochaete* spp., *E. antarctica* var. *antarctica*, *F. kerguelensis* and, with increasing depth, *Chaetoceros* resting spores. Stations C1 and C5, also on the plateau but southerly located, had reasonably different assemblages; station C1 in particular with its benthic species and bias for centrics, and C5 with its assemblage resembling the off-plateau HNLC station C11 assemblage. A common feature of these last two stations was the presence of *F. pseudonana* and *F. kerguelensis* as dominating species. Viewed by total biomass, the stations are divided into two distinct groups of high (Stations A3 and B5) and low (Stations C1, 5 and 11) biomass levels (Fig. 7), indicating that the plateau is not highly productive in all locations since Stations C1 and C5 were the least productive observed during our study. The temporal shift in biomass at Station A3 is discussed in Section 5. Geographical differences were in tune with the observations from the sea-floor diatom assemblage

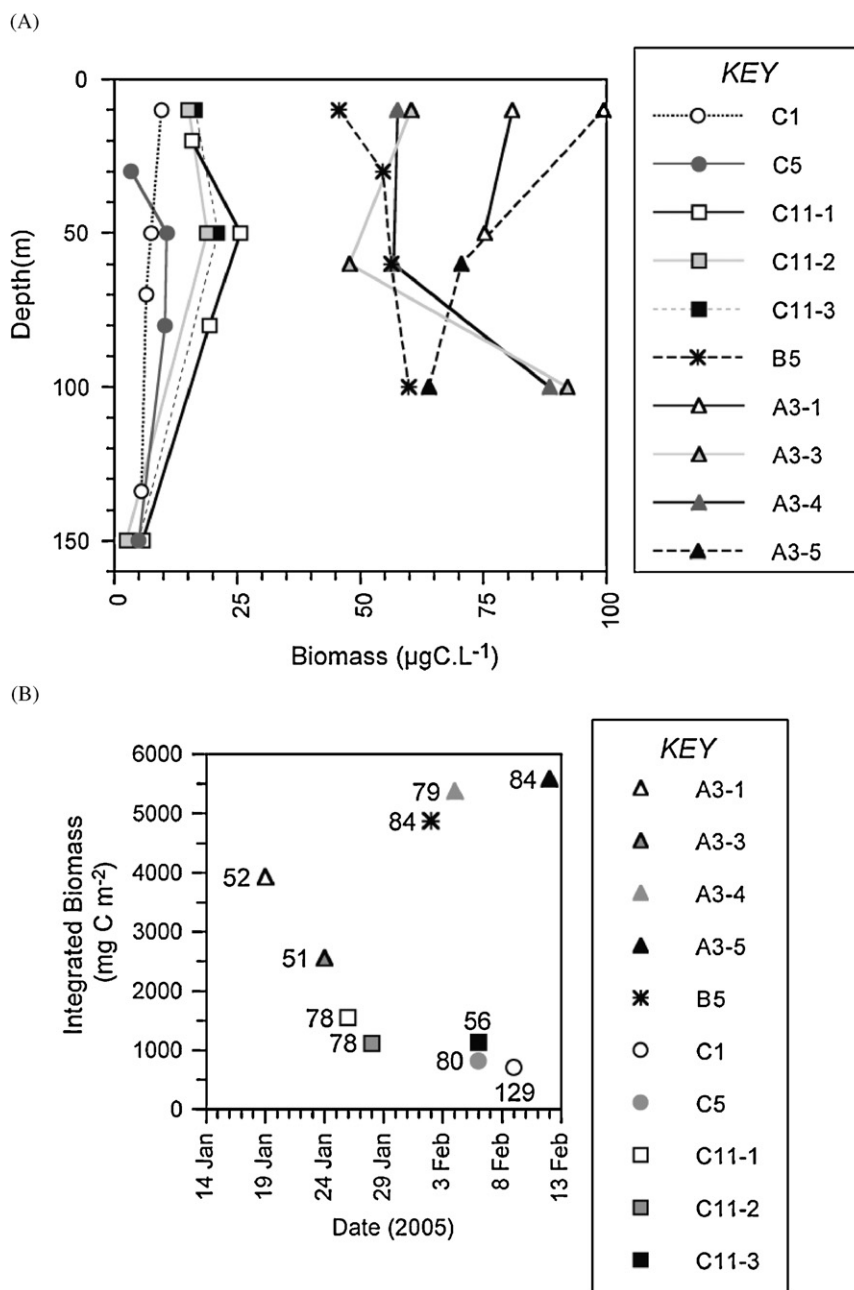


Fig. 7. Carbon biomass at KEOPS stations: (A) total carbon biomass by depth at all stations. Key indicates the relevant station visits. Stations are divided into low and high biomass groupings. (B) Mixed-layer depth-integrated diatom biomass over time. Depth of the mixed layer (m) at each site is identified on the plot. Key indicates the station and visit.

(Armand et al., 2008), where *Thalassionema nitz. f. nitzschoides*, *Chaetoceros* resting spores, *F. kerguelensis* and elevated *E. antarctica* abundances dominated over the plateau region, while typical open-ocean species, like *F. kerguelensis*, *T. lentiginosa* and *T. antarctica*, were found in the surface sediments below station C11.

4.3. Vertical distribution of biomass

The vertical profiles of diatom biomass at each CTD station are shown in Fig. 7A. Two of the three low biomass stations, C5 and C11, revealed a slight elevation in biomass

around 50 m depth from the surface values, which reduced towards or after 80 m and diminished to values $< 6 \mu\text{g CL}^{-1}$ by 150 m depth. In comparison, the KERFIX surface diatom biomass values during the summer maximum were considered poor, reaching $8.9 \mu\text{g CL}^{-1}$ (Kopczyńska et al., 1998). This value was closest to our poorest station surface estimates at C1 and C5, and essentially half the estimate obtained at Station C11 (Table 4). Direct comparison between our diatom-derived biomass estimates at Station C11 and those of various diatom proxy indicators, fucoxanthin, total Chl *a* and biogenic silica (Fig. 8), clearly reveal strong relationships,

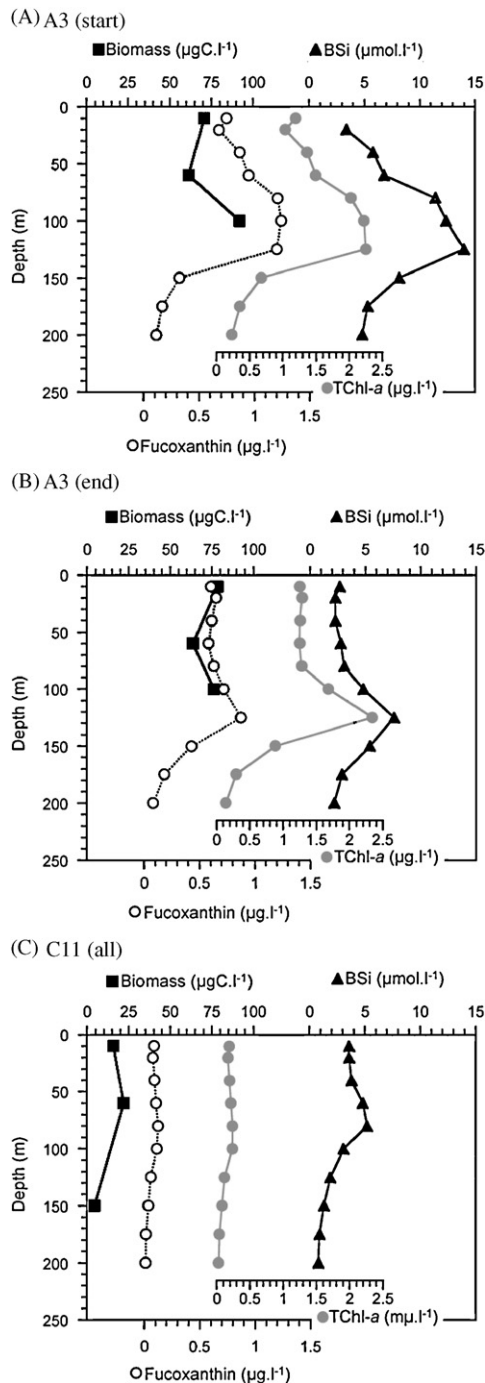


Fig. 8. Mean vertical profiles of biological parameters at A3 and C11. Mean values of biomass, fucoxanthin, total chlorophyll *a* (TChl *a*) and Biogenic silica (BSi) for stations A3 (start = first two visits and end = last two visits) and C11. Fucoxanthin and TChl *a* from Utiz et al. (submitted), BSi from Mosseri et al. (2008).

most closely with biogenic silica concentrations, and verify the proxy analyses as indirect indicators of the diatom contribution in the water column. We can use the proxies thus, to suggest that the major diatom biomass at C11 was located at a water depth between 80 and 100 m.

Station B5 and repeat station A3 both had large biomass contributions from 45.6 to 99.4 $\mu\text{g C L}^{-1}$ (Fig. 7A). These

values were greater than those reported around another Antarctic Island, Elephant Island (21–40 $\mu\text{g C L}^{-1}$, Villafane et al., 1993), or along the Polar Front in the South Atlantic (10–40 $\mu\text{g C L}^{-1}$, Smetacek et al., 2002). Unfortunately our sampling did not enable diatom biomass estimation deeper than 100 m, where we presume a decrease in biomass would have been encountered following the Chl *a* max below 125 m and as otherwise noted from data retrieved from HPLC analyses (Utiz et al., submitted, Fig. 8). Our biomass estimates at B5 increased steadily with depth climaxing at 100 m. A similar peak at 100 m was observed in two of the four repeat visits to A3, although estimates clearly decreased between the surface and the 100 m-depth peak (A3-3, A3-4). The last station visit to A3 revealed maximal abundances at the surface alone. This was a result of the >50% biomass input from atypical *E. antarctica* cells along with additional contributions from large cylindrical forms (*Proboscia*, *Corethron*, *Guinardia*) to the surface standing stock. Curiously, the 1% PAR level was found between 40 and 46 m at the B5 and A3 stations, which was well short of the maximum diatom biomass peak at 100 m. Evidence from the series of fucoxanthin, total Chl *a* and BSi analyses (Fig. 8) indicate the true diatom biomass maximum was most likely found between 80 and 130 m depth in the first half of the survey and only at 130 m depth during the last half of the sampling survey. The MLD for these stations was variable, being shallow (~51 m) in January and deeper (78–84 m) in February. Similarly, a bacterial biomass accumulation peak was also observed between 50 and 120 m, particularly on the third visit to Station A3 (Christaki et al., 2008).

The question is raised as to why various groups accumulated below the photic zone, especially when earlier studies in proximity to our study region suggest that biomass accumulation and large diatoms were related to prolonged surface water stability (Fiala et al., 1998) and that wind-induced vertical mixing provided uniform distribution of cells in the photic zone (Kopczyńska et al., 1986). Our assessment of living and non-viable cells at 100 m at our stations clearly indicate that the living community accounted for >78% of the total number of cells encountered (Fig. 3, A3 and B5). Although the pycnocline could be observed down to ~200 m (data not shown, Park et al., 2008b) an associated broad nutricline of both dissolved iron and silicic acid concentrations occurred within 125 and 150 m over the plateau (Blain et al., 2008; Mosseri et al., 2008) and could be an additional factor in the presence of elevated viable diatoms at depth. The fact that the dominant diatoms at Station A3 were notably more silicified and present as resting stages (e.g., single or doublet *E. antarctica* typical cells and *Chaetoceros* resting spores) in comparison to the surface assemblage raises the possibility of a dormant assemblage waiting for “improved environmental conditions” (Kemp et al., 2000).

Finally, we found that both size and abundance clearly do matter inequitably across species when determining biomass estimates. Small species only accounted for a

significant proportion of the standing stock when present in very high numbers, as illustrated in the following examples: At Station A3 more than 50% of the cellular count was required by *Chaetoceros Hyalochaete* spp. to achieve 20% of the biomass total. At C11 the same was true for *Fragilariopsis pseudonana*, with cellular abundances >50% required to account for >13% of the standing stock. Thus, in the case where community abundances were used in earlier studies to imply the contribution of diatom or phytoplankton biomass standing stocks from an alternatively derived biomass estimate (e.g., Chl *a* determined) caution is in order, since the inference is not supported by this study. Our results indicate that many rare or moderately abundant species were generally those that underpinned the biomass totals.

4.4. Integrated biomass

Integrated biomass estimates (Table 4) over the MLD are presented against time in Fig. 7B. The stations with highest integrated biomass increased their standing stock when the MLD deepened. The same is true over time at Station C11 where the highest integrated biomass was observed at the start of the survey prior to the MLD shallowing. In contrast to this trend, integrated biomass was very low with elevated MLD's at stations C1 and C5. The former, related specifically to its unique shallow environment and the latter potentially due to the disruptive influx of currents into the Heard–MacDonald Shoal via the northwestward trending Heard/MacDonald Islands Trough (Park et al., 2008b; van Beek et al., 2008).

Interestingly, the total standing stock over 80 m at EisenEx increased from 790 to 3508 mg C m⁻² inside the fertilised patch during their initiated bloom experiment (Assmy et al., 2007). Their values fell below our lowest estimates in the bloom Stations A3 and B5 (Table 4), nevertheless they remained larger than estimates produced for other stations on the plateau in a non-bloom state. The EisenEx integrated estimates outside the patch reached a maximum of 1150 mg C m⁻² during their survey period. This value sits extremely well within our evolving estimates of integrated biomass over the same depths at Station C11 (Table 4), however, our biomass extremes in this off-plateau HNLC region were not influenced as seriously by cylindrical-shaped species as was observed outside the patch during EisenEx.

5. Temporal changes in community composition at station A3

Our results indicate that a substantial change in the diatom community structure occurred at Station A3, where small and numerous *Chaetoceros Hyalochaete* spp. were replaced after the second visit (24 January) by *Eucampia ant. v. antarctica*. Mosseri et al. (2008) suggested from the examination of silicic acid uptake kinetics that the change from a *Chaetoceros* to an *Eucampia* dominated community

could be related to species affinities for silicic acid, which were higher for *E. antarctica*. This implies *Eucampia* has an enhanced ability to grow in low Si(OH)₄ waters.

Temporal changes also occurred in other components of the ecosystem aside from the change in diatom community structure at station A3. Christaki et al. (2008) observed the highest bacterial abundances over Station A3, with biomass substantially decreased between the first two and last two repeat visits. Bacterial biomass and production were found to be significantly correlated with phytoplankton biomass derived from integrated Chl *a* measurements (Christaki et al., 2008). Copepod abundances, subject to artefacts inherent in diel vertical migration, did not respond in the same manner before and after 30 January at Station A3, in fact abundances remained the same with a very minor decrease on 12 February (Carlotti et al., 2008). However, copepod gut pigment contents were noted to have changed from high to low phytoplankton consumption between the first two and last two visits. Finally, a distinct shift in the net community production from a previously dominant autotrophic to heterotrophic plankton metabolism was observed between the last two sampling events (Lefèvre et al., 2008).

The physical environment over A3 was subject to continuous tidal influenced semi-diurnal internal waves with subsequent vertical change in the MLD and enhanced vertical mixing (Park et al., 2008a). The injection of subsurface winter water, positioned at ~200 m depth and elevated in dissolved iron and silicic acid (Blain et al., 2008; Mosseri et al., 2008), via this vertical transport mechanism would serve as an intermittent and continuous nutrient inoculum in the otherwise deplete surface waters. A large storm event occurred on 3 January when winds were on average 31 ± 7 knots for 2.5 days. A deepening of the mixed layer due to the increased winds in conjunction with the effects of the internal waves makes it impossible for us to attribute a mechanism of physical change that may have lead to the transformation of the autotrophic assemblage between 24 January and 4 February.

Chemical analysis of the water column indicated silicic acid concentrations remained continuously low (~2 μmol L⁻¹) in contrast to the high nitrate concentrations in the surface waters (Mosseri et al., 2008). This chemical environment presents an interesting insight into either the formation and/or seeding of *Chaetoceros* resting spores as a bloom response species. We only observed *Chaetoceros* resting spores at depth in large numbers, and although the relative abundance of viable *Chaetoceros* resting spores remained in the 20% range, their abundance did increase slightly to 30% at 100 m-depth after the storm event (Appendix 3); a value equivalent to that observed maximally in experimental resting spore trigger studies (Kuwata and Takahashi, 1990).

The formation of *Chaetoceros* resting spores has been reported as an early response survival tactic to nutrient stress, typically related to nitrogen deficiency (Hargraves and French, 1983) and increasing the sinking rate 5 times

greater than in the vegetative form (Bienfang, 1981). Nitrogen was not limiting and unlikely as the spore trigger at KEOPS sites. Silicic acid and iron concentrations, however, in the surface waters were consistently low and may have been sufficient, with storm-induced mixing, to trigger an additional or final spore formation event. Another small *Chaetoceros Hyalochaete* species (*C. brevis*) had been shown to grow regardless of low iron conditions both during the KEOPS study and earlier experiments (Timmermans et al., 2001, 2008), deeming silicic acid availability as a control on population growth.

Our populations of *Chaetoceros* vegetative cells were unhealthy and no longer in chain formation by the end of the survey, as observed in experimental studies of resting spore formation affected by silica limitation (Kuwata and Takahashi, 1990). These authors concluded that the presence of both resting spores and unhealthy vegetative cells provided two mechanisms of survival in regions of pulsed nutrient supply; unhealthy vegetative cells respond immediately to short-term nutrient supply and resting spores to longer-term nutrient availability. Garrison (1984) raised the idea that resting spores provided a short-term survival strategy where mixing events periodically interrupt stratification and thus repeated blooms could continue through a seasonal cycle through rapid resuspension. This hypothesis is a likely scenario for our Station A3 observations, and supports the observations (Pitcher, 1986; Ferrario et al., 1998) and hypothesis (Smetacek, 1985) of a “seeding” population below the pycnocline. Our observations suggest the supply of increased nutrient concentrations from below, particularly silicic acid, as a trigger for *Chaetoceros Hyalochaete* species germination with concurrent spore resuspension. Our observations lend support to the idea of nutrient-stress-induced changes in the diatom community in response to presumably regular punctuated physico-chemical variation over the plateau and the influence of a wind-forced MLD.

The subsequent *E. antarctica* bloom development at Station A3, gave rise to an atypical *E. antarctica* community in the surface waters and a typical form at 100 m (Fig. 2). *Eucampia antarctica* had not been identified as a major bloom forming species and, within the Kerguelen region, was generally reported as sporadic or in low numbers (Jacques et al., 1979; Fiala et al., 1998; Kopczyńska et al., 1998). Elsewhere in the Southern Ocean, at South Georgia Island, the species has been reported as a dominant constituent (Froneman et al., 1997; Ward et al., 2006). In the latter of the two studies at South Georgia *E. antarctica* and *Corethron* (as *C. criophilum*) were observed as widely co-occurring species and presumably stimulated by the influx of warmer Subantarctic surface waters (Froneman et al., 1997). The A3 surface water community was also composed of large cylindrical form species with small surface to volume ratios (Cornet-Barthaux et al., 2007) presumably making them ill-adapted for nutrient uptake in the $\text{Si}(\text{OH})_4$ -depleted waters. Smetacek (1985) speculates that large, un-ornamented

diatoms with a potentially large vacuole size, improve their positive buoyancy and ability for vertical migration between the nutricline and photic zone. This may be the scenario for the post-storm diatom surface assemblage we see after the depression of the MLD. In effect, the diatoms in the photic zone are all lightly silicified and preferentially smooth walled forms, including the atypical *E. antarctica* cells (Fig. 2). In the case of *E. antarctica*, the heavily silicified and intricate frustule design appears to have been minimised in aid of improved buoyancy and potentially reduced surface to volume ratio for nutrient uptake.

6. Comparison to previous studies

6.1. Cell densities and biomass

Cell abundances from earlier studies in the southwest Indian sector of the Southern Ocean vary dependent on methodology, integration depth or season. Average cell densities from our stations are listed in Table 4, and range from 4.3×10^4 cells L^{-1} at Station C1 to 53.9×10^4 cells L^{-1} at Station A3-1. Our lowest values are closest to the highest surface values ($2.3\text{--}4.9 \times 10^4$ cells L^{-1}) reported by Blain et al. (2001) in their off-plateau, high iron and stable light-mixing environment. This difference is large in contrast to our bloom samples and we assume that a higher cell density may have been observed with deeper photic zone sampling in their Zone 3. At the fixed station KERFIX, west of Kerguelen Plateau, summer cell densities ranged from 2.3 to 17.5×10^4 cells L^{-1} (Fiala et al., 1998; Kopczyńska et al., 1998); again these values remained lower than the summer values we observed over our HNLC station C11, where our values were 1.2–2.6 times greater, yet are similar to the values observed at Station C5 at the south-eastern border of the Kerguelen Plateau (Table 4).

High depth-integrated cell densities have nevertheless been reported from the Polar Front in the southwest Indian Ocean. Steyaert (1973) observed 33.6×10^4 cells L^{-1} , whereas Kopczyńska et al. (1986) observed 99×10^4 cells L^{-1} , both studies identifying 50 or 70 m depth as the zone of greatest cell density. Our results at C11 and C5 support this finding of higher cell abundances at depth, whereas plateau stations were far more homogeneous in the surface layers (Fig. 3).

The experimental, Polar Front eddy, EisenEx study reported elevated cell densities integrated over 80 m of up to 44.4×10^4 cells L^{-1} as a result of iron fertilisation after 3 weeks (Assmy et al., 2007). This estimate is within the highest values obtained at Station A3, but remains also within the numbers averaged over 80 m at C11 in our study (Table 4). The EisenEx out of patch values are 2.8–5.6 times lower than our C11 observations. Whether this implies that our HNLC station experienced bloom conditions or was influenced by physio-chemical conditions leeward of the plateau cannot be determined without studying winter background diatom levels.

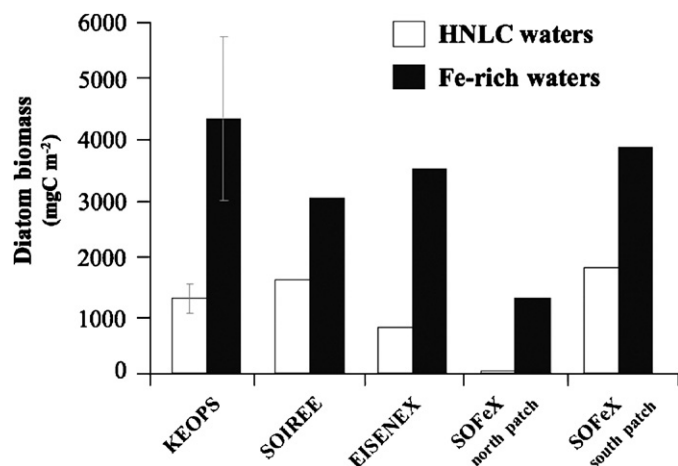


Fig. 9. Comparison of total biomass values between this and Fe fertilisation studies. Diatom carbon biomass integrated within the mixed layer in Fe-enriched and HNLC waters of the Southern Ocean Fe studies: KEOPS (this study), SOIREE (Gall et al., 2001), EisenEx (Assmy et al., 2007), SOFeX (Coale et al., 2004). The biomass in Fe-enriched waters was taken from Station A3 (averaged over the four visits) for the KEOPS program while it was taken from the final conditions of each experiment for the mesoscale Fe-enrichment experiments. The biomass in HNLC waters was taken from the station C11 (averaged over the three visits) for the KEOPS program while it was taken from the initial conditions of each experiment for the mesoscale Fe-enrichment experiments.

In all mesoscale Fe-fertilisation experiments, the diatom biomass observed after iron enrichment clearly contrasted with the HNLC initial conditions prevailing at the beginning of Fe additions. The diatom carbon biomass measured during the KEOPS study is compared with these artificially Fe-enriched diatom patches in the Southern Ocean in Fig. 9. In the mixed layer, the diatom carbon biomass of the Kerguelen Plateau was not statistically different to other Fe-enriched waters, although it attained one of the highest levels of C biomass. This comparison does not take into account the large biomass accumulated below the mixed layer in the KEOPS study.

6.2. Species/community differences with iron addition

The low abundance of *F. kerguelensis* in the Kerguelen bloom contrasts with the SOIREE artificial iron fertilisation in the open ocean (Gall et al., 2001). Assmy et al. (2006, 2007) considered *F. kerguelensis* as a slow growing species along with *Thalassionema nitzschioides*, with both species being representative of Fe depleted environments. Timmermans et al. (2004) put such increased responses in *F. kerguelensis* down to the lower requirement of Fe to stimulate this diatom species growth in comparison to other larger species. *F. kerguelensis* was nevertheless important both inside the bloom at A3 and outside at C11 because, as at EisenEx (Assmy et al., 2007), it was one of the major biomass contributors. Assmy et al. (2006) found that Fe-aided stimulation of the natural sexual phase of *F. kerguelensis* leading to the size definition for newly formed initial cells (76–90 μm). We did not observe size-

related evidence of a recent sexual phase at our bloom station, A3, either before or after the change in species community (data not shown). Most of our specimens were in the 20–58 μm size range, most likely indicative of an aged population. At Station C11 very small numbers of *F. kerguelensis* cells greater than 76 μm were observed. These large cells were encountered on the first visit to C11 in the 20–50 m samples, possibly indicating a recent sexual size restoration event prior to our arrival. The remainder of the specimens were slightly larger than the populations observed at Station A3. Chain length of *F. kerguelensis* was not studied in great detail due to the biased affect of CTD sampling (i.e. shorter chains to that observed in net haul samples, breakage of chains prior to lab assessment). Nevertheless, a small subset of CTD-based observations over the course of the study indicated chain length at Station A3 was longer at the first two visits (average 7 cells chain⁻¹) than the last two (average 2 cells chain⁻¹). At the HNLC Station, C11, chain length was longer (average 8 cells chain⁻¹) but decreased by the end of the survey (average 5 cells chain⁻¹).

Hyalochaete Chaetoceros blooms have been observed in artificial iron experiments carried out in the subarctic Pacific, with *Chaetoceros debilis* responsible for the massive iron-mediated bloom reported during SEEDS (Tsuda et al., 2004) and *Chaetoceros* spp. forming an early bloom and decline species after iron addition during SERIES (Boyd et al., 2005). As discussed previously, the bloom response over Station A3 appears to have been dominated prior to our arrival by *Chaetoceros Hyalochaete* spp., the partial remains of which are most likely stocked in the subsurface maximum diatom biomass layer. We assume that the small *Chaetoceros Hyalochaete* spp. were the major bloom species during the seasonal phytoplankton increase. We also believe that the role of spore formation was triggered with the depletion of silicic acid. Unhealthy vegetative cells (cellular contents considerably diminished, previous chained assemblages reduced to single cells or a few in a chain) left at the end of the bloom particularly after 24 January were either due to zooplankton grazing, natural cell death or viral lysis. These cells also may have been the remnants of rapid growth unable to produce spores (as observed by Kuwata and Takahashi, 1990) and thus dependent on the punctuated influx of nutrients by physical processes, unique to the plateau, for continued survival.

Pseudo-nitzschia spp. did not play an important role in the KEOPS study region either on or off-plateau. At best, *Pseudo-nitzschia* spp. (<5 μm) appeared as a background species elevated in abundance with depth at A3, C11 and C5 stations. This is in contrast to experimental Fe studies elsewhere in the Southern Ocean (SOFEX, Eifex, EisenEx, de Baar et al., 2005). The observations from SEEDS in the Subarctic Pacific (Tsuda et al., 2004) may be closest to the events at Kerguelen with a replacement of a *Pseudo-nitzschia*-dominated community to a *Chaetoceros Hyalochaete* spp. bloom on addition of Fe. This assumes that the

Kerguelen bloom maximum is *Chaetoceros* dominated at it's peak and that dominances of *Pseudo-nitzschia* species (*P. heimii*, *P. lineola*) previously noted in summer surface waters at KERFIX (Kopczyńska et al., 1998) are less competitive with greater Fe supply.

7. Conclusions

Diatom communities and biomass contributions were considerably different within and external to the iron-enriched plateau, and species abundance alone could not account for the major carbon biomass contributor species at any site. Floristic succession was observed over the plateau with the loss of the smaller *Hyalochaete Chaetoceros* spp. and the development of a remnant *E. antarctica* population towards the end of the bloom at Station A3. The diatom community at C11, outside of the bloom region, showed little change over 25 days, remaining distinct from the bloom community over the plateau. These differences in the two regions also were observed in diatom signatures preserved on the sea-floor (Armand et al., 2008). The diatom observations and combined indices also clearly point to a subsurface maximum of diatom biomass. At the HNLC stations (C11) this biomass peak was situated at ~80–100 m. Biomass peaks at 80–130 m depth at the bloom stations A3 and B5 were considerably below the 1% PAR depth and the MLD, and likely related to the iron and silicic acid nutricline (i.e. 125–150 m depth) and the sinking of cells and resting spores from the surface. The surface waters 0–100 m were dominated by the living fraction whereas indications from the 150 m sample at C11 and the diatom biomass indices of biogenic silica, total Chl *a* and fucoxanthin, suggest the diatom assemblage was increasingly senescent below 150 m.

The change in community structure over time at the A3 plateau site suggests links between nutrient availability and diatom ecological responses. *Chaetoceros Hyalochaete* spp. demise and spore formation and *E. antarctica* changes in morphology provided tantalizing glimpses into possible life cycle strategies taken by these diatoms in response to interrupted nutrient supply. The role of wind-forced mixed-layer deepening in conjunction with vertical mixing requires further investigation to determine the ultimate interplay between nutrient sources and light limitations on the Kerguelen bloom ecosystem structure.

Acknowledgments

This work was undertaken and supported by a European Union FP6 Marie Curie International Incoming Fellowship carried out at the Centre d'Océanologie de Marseille, France, awarded to LA. We expressly thank the KEOPS PI Prof. S. Blain, Commandant Heidrich, the crew and scientific personnel aboard the R.V. *Marion Dufresne II*, during the mission. Drs. F. Carlotti, D. Vincent, and Ms. A. Jaeger are gratefully acknowledged with assisting in the

sampling and/or qualitative assessment of net hauled material. Dr. P. Bonham (CMAR-Hobart) enlightened us on the use of Sedgwick–Rafter chambers. Two anonymous reviewers and the sub-editor T. Trull provided positive constructive commentary that enhanced the manuscript.

Appendix A. Supplementary Materials

Supplementary data associated with this article can be found in the online version at [doi:10.1016/j.dsr2.2007.12.031](https://doi.org/10.1016/j.dsr2.2007.12.031).

References

- Armand, L.K., Crosta, X., Quéguiner, B., Mosseri, J., Garcia, N., 2008. Diatoms in surface sediments of the Kerguelen-Heard region of the South Indian Ocean. *Deep-Sea Research II*, this issue [[doi:10.1016/j.dsr2.2007.12.031](https://doi.org/10.1016/j.dsr2.2007.12.031)].
- Assmy, P., Henjes, J., Smetacek, V., Montresor, M., 2006. Auxospore formation by the silica-sinking, oceanic diatom *Fragilariopsis kerguelensis* (Bacillariophyceae). *Journal of Phycology* 42, 1002–1006.
- Assmy, P., Henjes, J., Klaas, C., Smetacek, V., 2007. Mechanisms determining species dominance in a phytoplankton bloom induced by the iron fertilization experiment EisenEx in the Southern Ocean. *Deep-Sea Research I* 54 (3), 340–362.
- Bienfang, P.K., 1981. Sinking rates of heterogeneous, temperate phytoplankton populations. *Journal of Plankton Research* 3 (2), 235–253.
- Blain, S., Tréguer, P., Belviso, S., Bucciarelli, E., Denis, M., Desabre, S., Fiala, M., Martin-Jézéquel, V., Le Fèvre, J., Mayzaud, P., Marty, J.-C., Razouls, S., 2001. A biogeochemical study of the island mass effect in the context of the iron hypothesis: Kerguelen Islands, Southern Ocean. *Deep-Sea Research I* 48, 163–187.
- Blain, S., Quéguiner, B., Armand, L., Belviso, S., Bombled, B., Bopp, L., Bowie, A., Brunet, C., Brussaard, C., Carlotti, F., Christaki, U., Corbière, A., Durand, I., Ebersbach, F., Fuda, J.-L., Garcia, N., Gerringa, L., Griffiths, B., Guigüe, C., Guillermin, C., Jacquet, S., Jeandel, C., Laan, P., Lefèvre, D., Lomonaco, C., Malits, A., Mosseri, J., Obernosterer, I., Park, Y.-H., Picheral, M., Pondaven, P., Remy, T., Sandroni, V., Sarthou, G., Savoye, N., Scouarnec, L., Souhaut, M., Thuiller, D., Timmermans, K., Trull, T., Uitz, J., van-Beek, P., Veldhuis, M., Vincent, D., Viollier, E., Vong, L., Wagener, T., 2007. Impacts of natural iron fertilisation on the Southern Ocean. *Nature* 446, 1070–1074.
- Blain, S., Sarthou, G., Laan, P., 2008. Distribution of dissolved iron during the natural iron fertilization experiment KEOPS (Kerguelen Island, Southern Ocean). *Deep-Sea Research II*, this issue [[doi:10.1016/j.dsr2.2007.12.031](https://doi.org/10.1016/j.dsr2.2007.12.031)].
- Boyd, P.W., Strzepek, R., Takeda, S., Jackson, G., Wong, C.S., McKay, R.M., Law, C., Kiyosawa, H., Saito, H., Sherry, N., Johnson, K., Gower, J., Ramaiah, N., 2005. The evolution and termination of an iron-induced mesoscale bloom in the northeast subarctic Pacific. *Limnology and Oceanography* 50 (6), 1872–1886.
- Bucciarelli, E., Blain, S., Tréguer, P., 2001. Iron and manganese in the wake of the Kerguelen Islands (Southern Ocean). *Marine Chemistry* 73, 21–36.
- Carlotti, F., Thibault-Botha, D., Nowaczyk, A., Lefèvre, D., 2008. this volume. Zooplankton community structure, biomass and role in carbon transformation during the second half of a phytoplankton bloom on the eastern part of the Kerguelen Plateau (January–February 2005). *Deep-Sea Research II*, this issue [[doi:10.1016/j.dsr2.2007.12.031](https://doi.org/10.1016/j.dsr2.2007.12.031)].
- Charrassin, J.-B., Park, Y.-H., Le Majo, Y.L., Bost, C.-A., 2004. Fine resolution 3D temperature fields off Kerguelen from instrumented penguins. *Deep-Sea Research I* 51 (12), 2091–2103.

- Christaki, U., Obernosterer, I., Van Wambeke, F., Veldhuis, M.J.W., Garcia, N., Catala, P., 2008. Microbial food web structure in a naturally iron fertilized area in the Southern Ocean (Kerguelen Plateau). *Deep-Sea Research II*, this issue [doi:10.1016/j.dsr2.2007.12.031].
- Coale, K.H., Johnson, K.S., Chavez, F.P., Buesseler, K.O., Barber, R.T., Brzezinski, M.A., Cochlan, W.P., Millero, F.J., Falkowski, P.G., Bauer, J.E., Wanninkhof, R.H., Kudela, R.M., Altabet, M.A., Hales, B.E., Takahashi, T., Landry, M.R., Bidigare, R.R., Wang, X., Chase, Z., Strutton, P.G., Friederich, G.E., Gorbunov, M.Y., Lance, V.P., Hilting, A.K., Hiscock, M.R., Demarest, M., Hiscock, W.T., Sullivan, K.F., Tanner, S.J., Gordon, R.M., Hunter, C.N., Elrod, V.A., Fitzwater, S.E., Jones, J.L., Tozzi, S., Koblizek, M., Roberts, A.E., Herndon, J., Brewster, J., Ladizinsky, N., Smith, G., Cooper, D., Timothy, D., Brown, S.L., Selph, K.E., Sheridan, C.C., Twining, B.S., Johnson, Z.I., 2004. Southern Ocean iron enrichment experiment: carbon cycling in high- and low-Si waters. *Nature* 304, 408–414.
- Cornet-Barthaux, V., Armand, L., Quéguiner, B., 2007. Biovolume and biomass measurements of key Southern Ocean diatoms. *Aquatic Microbial Ecosystems* 48, 295–308.
- de Baar, H.J.W., Boyd, P.W., Coale, K.H., Landry, M.R., Tsuda, A., Assmy, P., Bakker, D.C.E., Bozec, Y., Barber, R.T., Brzezinski, M.A., Buesseler, K.O., Boyé, M., Croot, P.L., Gervais, F., Gorbunov, M.Y., Harrison, P.J., Hiscock, W.T., Laan, P., Lancelot, C., Law, C.S., Lavasseur, M., Marchetti, A., Millero, F.J., Nishioka, J., Nojiri, Y., Van Oijen, T., Riebesell, U., Rijkenberg, M.J.A., Saito, H., Takeda, S., Timmermans, K.R., Veldhuis, M.J.W., Waite, A.M., Wong, C.-S., 2005. Synthesis of iron fertilization experiments: from the iron age in the age of enlightenment. *Journal of Geophysical Research* 110.
- Ealey, E.H.M., Chittleborough, R.G., 1956. Plankton, hydrology and marine fouling at Heard Island. In: Law, P. (Ed.), *Australian National Antarctic Research Expeditions Interim Report 15*, Melbourne, p. 81.
- Ferrario, M.E., Sar, E.A., Vernet, M., 1998. *Chaetoceros* resting spores in the Gerlache Strait, Antarctic Peninsula. *Polar Biology* 19, 286–288.
- Fiala, M., Kopczyńska, E.E., Jeandel, C., Oriol, L., Vétion, G., 1998. Seasonal and interannual variability of size-fractionated phytoplankton biomass and community structure at station Kerfix, off Kerguelen Islands, Antarctica. *Journal of Plankton Research* 20 (7), 1341–1356.
- Froneman, P.W., Pakhomov, E.A., Laubscher, R.K., 1997. Microphytoplankton assemblages in the waters surrounding South Georgia, Antarctica during austral summer 1994. *Polar Biology* 17, 515–522.
- Fryxell, G.A., 1991. Comparison of winter and summer growth stages of the diatom *Eucampia antarctica* from the Kerguelen Plateau and south of the Antarctic Convergence Zone. In: Barron, J., Larsen, B., et al. (Eds.), *Proceedings of the Ocean Drilling Program, Scientific Results. Ocean Drilling Program, College Station, TX*, pp. 675–685.
- Fryxell, G.A., 1994. Planktonic marine diatom winter stages: Antarctic alternatives to resting spores. *Memoirs of the California Academy of Sciences* 17, 437–448.
- Gall, M.P., Boyd, P.W., Hall, J., Safi, K.A., Chang, H., 2001. Phytoplankton processes. Part 1: Community structure during the Southern Ocean Iron RElease Experiment (SOIREE). *Deep-Sea Research II* 48, 2551–2570.
- Garrison, D.L., 1984. Planktonic Diatoms. In: Steidinger, K.A., Walker, L.M. (Eds.), *Marine Plankton Life Cycle Strategies*. CRC Press Inc., Boca Raton, FL, pp. 1–17.
- Guillard, R.R.L., 1978. Counting slides. In: Sournia, A. (Ed.), *Phytoplankton Manual*. UNESCO, Paris, pp. 182–189.
- Hargraves, P.E., French, F.W., 1983. Diatom resting spores: significance and strategies. In: Fryxell, G. (Ed.), *Survival Strategies of the Algae*. Cambridge University Press, Cambridge, pp. 49–68.
- Hasle, G., 1978. Using the inverted-microscope method. In: Sournia, A. (Ed.), *Phytoplankton Manual*. UNESCO, Paris, pp. 191–196.
- Hasle, G.R., Syvertsen, E.E., 1997. Marine diatoms. In: Tomas, C.R. (Ed.), *Identifying Marine Phytoplankton*. Academic Press, New York, pp. 5–361.
- Hötzel, G., Croome, R., 1998. A phytoplankton methods manual for Australian Rivers (Occasional Paper 18/98), Land and Water Research and Development Corporation, Canberra, p. 52.
- Jacques, G., Descolas-Gros, C., Grall, J.-R., Sournia, A., 1979. Distribution du phytoplancton dans la partie Antarctique de l’Océan Indien en fin d’été. *Internationale Revue der Gesamten Hydrobiologie* 64 (5), 609–628.
- Jeffery, S.W., Mantoura, R.F.C., Wright, S.W., 2005. *Phytoplankton Pigments in Oceanography. Guidelines to Modern Methods*. UNESCO Publishing, Paris.
- Kemp, A.E.S., Pearce, R.B., Grigorov, I., Rance, J., Lange, C.B., Quilty, P., Salter, I., 2006. Production of giant marine diatoms and their export at oceanic frontal zones: implications for Si and C flux from stratified oceans. *Global Biogeochemical Cycles* 20.
- Kopczyńska, E.E., Weber, L.H., El-Sayed, S.Z., 1986. Phytoplankton species composition and abundance in the Indian Sector of the Antarctic Ocean. *Polar Biology* 6, 161–169.
- Kopczyńska, E.E., Fiala, M., Jeandel, C., 1998. Annual and interannual variability in phytoplankton at a permanent station off Kerguelen Islands, Southern Ocean. *Polar Biology* 20, 342–351.
- Kopczyńska, E.E., Fiala, M., 2003. Surface phytoplankton composition and carbon biomass distribution in the Crozet Basin during austral summer of 1999: variability across frontal zones. *Polar Biology* 27, 17–28.
- Kozlova, O.G., 1962. Specific composition of diatoms in the waters of the Indian sector of the Antarctic. *Trudy Instituta Okeologii. Akademiya Nauk SSSR* 61, 3–18.
- Kuwata, A., Takahashi, M., 1990. Life-form population responses of a marine planktonic diatom, *Chaetoceros pseudocurvisetus*, to oligotrophication in regionally upwelled water. *Marine Biology* 107, 503–512.
- Lefèvre, D., Guigue, C., Obernosterer, I., 2008. The metabolic balance at two contrasting sites in the Southern Ocean: above the kerguelen plateau and in open ocean waters. *Deep-Sea Research II*, this issue [doi:10.1016/j.dsr2.2007.12.031].
- Manguin, E., 1954. Diatomés marines provenant de l’île Heard (Australian National Research Expedition). *Revue Algologique (nouvelle Série)* 1 (1), 14–24.
- Mongin, M., Molina, E., Trull, T., 2008. Seasonality and scale of the Kerguelen plateau phytoplankton bloom: a remote sensing and modeling analysis if the influence of natural iron fertilization in the Southern Ocean. *Deep-Sea Research II*, this issue [doi:10.1016/j.dsr2.2007.12.031].
- Mosseri, J., Quéguiner, B., Armand, L., Cornet-Barthaux, V., 2008. Impact of iron on silicon utilization by diatoms in the southern ocean: a case of Si/N cycle decoupling in a naturally iron-enriched area. *Deep-Sea Research II*, this issue [doi:10.1016/j.dsr2.2007.12.031].
- O’Meara, E., 1877. On the diatomaceous gatherings made at Kerguelen’s Land by H.N. Moseley, M.A., H.M.S. “Challenger”. *Journal of the Linnean Society (Botany)* XV (82), 55–59 Plate I.
- Obernosterer, I., Christaki, U., Lefèvre, D., Catala, P., Van Wambeke, F., Le Baron, P., 2008. Rapid bacterial remineralization of organic carbon produced during a phytoplankton bloom induced by natural iron fertilization in the Southern Ocean. *Deep-Sea Research II*, this issue [doi:10.1016/j.dsr2.2007.12.031].
- Park, Y.-H., Gambéroni, L., 1995. Large-scale circulation and its variability in the south Indian Ocean from TOPEX/POSEIDON altimetry. *Journal of Geophysical Research* 100 (C12), 24, 911–924, 929.
- Park, Y.-H., Gambéroni, L., 1997. Cross-frontal exchange of Antarctic Bottom Water in Crozet Basin. *Deep-Sea Research II* 44 (5), 963–986.
- Park, Y.-H., Gambéroni, L., Charriaud, E., 1991. Frontal structure and transport of the Antarctic Circumpolar Current in the South Indian Ocean sector, 40–80°E. *Marine Chemistry* 35, 45–62.
- Park, Y.-H., E., C., Fieux, M., 1998. Thermohaline structure of the Antarctic surface water/winter water in the Indian sector of the Southern Ocean. *Journal of Marine Systems* 17, 5–23.
- Park, Y.H., Fuda, J.L., Durand, I., Naveira Garabato, A.C., 2008a. Internal tides and vertical mixing over the Kerguelen Plateau. *Deep-Sea Research II*, this issue [doi:10.1016/j.dsr2.2007.12.031].

- Park, Y.H., Roquet, F., Durand, I., Fuda, J.L., 2008b. Large scale circulation over and around the Northern Kerguelen Plateau. Deep-Sea Research II, this issue [doi:10.1016/j.dsr2.2007.12.031].
- Pitcher, G.C., 1986. Sedimentary flux and the formation of resting spores of selected *Chaetoceros* species at two sites in the Southern Benguela System. South African Journal of Marine Science 4, 231–244.
- Round, F.E., Crawford, R.M., Mann, D.G., 1990. The Diatoms. Biology & Morphology of the Genera. Cambridge University Press, Cambridge.
- Schlitzer, R., 2006. Ocean data view. <<http://odv.awi.de>>.
- Smetacek, V., 1985. Role of sinking in diatom life-history cycles: ecological, evolutionary and geological significance. Marine Biology 84, 239–251.
- Smetacek, V., Klaas, C., Menden-Deuer, S., Rynearson, T.A., 2002. Mesoscale distribution of dominant diatom species relative to the hydrographical field along the Antarctic Polar Front. Deep-Sea Research II 49, 3835–3848.
- Sournia, A., Grall, J.-R., Jacques, G., 1979. Diatomées et Dinoflagelles planctoniques d'une coupe meridienne dans le sud de L'Océan Indien (campagne Antipod I du *Marion-DuFresne*, mars 1977) (Plankton diatoms and dinoflagellates along a Meridian transect in the Southern Indian Ocean (Cruise Antipod I of the R/V "*Marion DuFresne*" March 1977). Botanica Marina XXII, 183–198.
- Steyaert, J., 1973. Distribution of plankton diatoms along an African–Antarctic transect. Investigaciones Pesqueras 37 (2), 295–328.
- Steyaert, J., 1974. Distribution of some selected diatom species during the Belgo-Dutch Antarctic expedition of 1964–65 and 1966–67. Investigaciones Pesqueras 38 (2), 259–287.
- Sullivan, C.W., Arrigo, K.R., McClain, C.R., Comiso, J.C., Firestone, J., 1993. Distributions of phytoplankton blooms in the Southern Ocean. Science 262, 1832–1837.
- Timmermans, K.R., Davey, M.S., van der Wagt, B., Snoek, J., Geider, R.J., Veldhuis, M.J.W., Gerringa, L.J.A., de Baar, H.J.W., 2001. Co-limitation by iron and light of *Chaetoceros brevis*, *C. dichaeta* and *C. calcitrans* (Bacillariophyceae). Marine Ecology Progress Series 217, 287–297.
- Timmermans, K.R., van der Wagt, B., de Baar, H.J.W., 2004. Growth rates, half-saturation constants, and silicate, nitrate, and phosphate depletion in relation to iron availability of four large, open-ocean diatoms from the Southern Ocean. Limnology and Oceanography 49 (6), 2141–2151.
- Timmermans, K.R., Veldhuis, M.J.W., Brussaard, C.P.D., 2008. Probing natural iron fertilization near the Kerguelen (Southern Ocean) using natural phytoplankton assemblages and diatoms cultures. Deep-Sea Research II, this volume [doi:10.1016/j.dsr2.2007.12.031].
- Tsuda, A., Takeda, S., Saito, H., Nishioka, J., Nojiri, Y., Kudo, I., Kiyosawa, H., Shiimoto, a., Imai, K., Ono, T., Shimamoto, A., Tsumune, D., Yoshimura, T., Aono, T., Hinuma, A., Kingasa, M., Suzuki, K., Sohrin, Y., Noiri, Y., Tani, H., deguchi, Y., Tsurushima, N., Ogawa, H., Fukami, K., Kuma, K., Saino, T., 2004. A mesoscale iron enrichment in the western subarctic Pacific induces a large centric diatom bloom. Science 300, 958–961.
- Uitz, J., Claustre, H., Garcia, N., Griffiths, B., Ras, V., Sandroni, V., submitted. A phytoplankton class-specific primary production model applied to the Kerguelen Islands region (Southern Ocean). Deep-Sea Research I (under revision).
- Van Beek, P., Bourquin, M., Reyss, J.L., Souhault, M., Charette, M., Jeandel, C., 2008. Radium isotopes to investigate the water mass pathways on the Kerguelen Plateau (Southern Ocean). Deep-Sea Research II, this issue [doi:10.1016/j.dsr2.2007.12.031].
- Villafane, V.E., Helbling, E.W., Holm-Hansen, O., 1993. Phytoplankton around Elephant Island, Antarctica. Polar Biology 13, 183–191.
- Ward, P., Shreeve, R., Aktkinson, A., Korb, B., Whitehouse, M., Thorpe, S., Pond, D., Cunningham, N., 2006. Plankton community structure and variability in the Scotia Sea: austral summer 2003. Marine Ecology Progress Series 309, 75–91.